

Electrowetting and Droplet Transport in Digital Microfluidic Chips for Mixing Applications

Shaik Faruk Azam

A Dissertation Submitted to
Indian Institute of Technology Hyderabad
In Partial Fulfillment of the Requirements for
The Degree of Master of Technology



भारतीय प्रौद्योगिकी संस्थान हैदराबाद
Indian Institute of Technology Hyderabad

Department of Biomedical Engineering

June, 2015

Declaration

I declare that this written submission represents my ideas in my own words, and where others' ideas or words have been included, I have adequately cited and referenced the original sources. I also declare that I have adhered to all principles of academic honesty and integrity and have not misrepresented or fabricated or falsified any idea/data/fact/source in my submission. I understand that any violation of the above will be a cause for disciplinary action by the Institute and can also evoke penal action from the sources that have thus not been properly cited, or from whom proper permission has not been taken when needed.



(Signature)

Shaik Faruk Azam


(Student Name)

BM13M1006

(Roll No)

Approval Sheet

This thesis entitled 'Electrowetting and Droplet Transport in Digital Microfluidic Chips for Mixing Applications' by Shaik Faruk Azam is approved for the degree of Master of Technology from IIT Hyderabad.



Dr. Subha Narayan Rath
Assistant Professor
Department of Biomedical Engineering
Indian Institute of Technology, Hyderabad
Examiner



Dr. Harikrishnan Narayanan Unni
Assistant Professor
Department of Biomedical Engineering
Indian Institute of Technology, Hyderabad
Advisor



Dr. Janardhanan, Vinod
Associate Professor
Department of Chemical Engineering
Indian Institute of Technology, Hyderabad
Chairman

Acknowledgements

I express my sincere gratitude to supervisor, respected Dr. Harikrishnan Narayanan Unni, under whose esteemed guidance and supervision, this work has been completed. This project work would have been impossible to carry out without his motivation and support throughout.

I am grateful to the Micro-Fluidic lab of the Department of Biomedical Engineering, IIT Hyderabad for providing an excellent environment for carrying out the project work.

Dedicated to

This thesis is dedicated to my inspiring parents,
who have raised me to be the person I am today.

What I have and will accomplish, is only possible due to
their unconditional love, guidance, support and sacrifices.

Also, this thesis is dedicated to my teachers,
who have always been a great source of motivation and inspiration.

And to all my loving friends.

Abstract

Microfluidics-based biochips have various applications like high throughput analyses, DNA sequencing, automated drug discovery, real time bio-molecular recognition, parallel immunoassays, single cell studies and protein RNA interaction and environmental toxicity monitoring. Based upon the fluid flow pattern microfluidic-based devices can be categorized in two types. They are continuous flow microfluidic device and discrete flow microfluidic device or digital microfluidic. The continuous flow uses permanently etched microchannels, micro-pumps, and micro-valves for the application such as mixing, splitting, and transportation. In contrast to this discrete type flow uses array of electrodes, voltage to controlled droplet independently for the same application. The advantages of discrete type flow over continuous type are dynamic reconfigurability, reusable, control parameters are in electric domain, no mechanical parts and fault tolerance. The principle of electrowetting is used to deform and to actuate the droplet. The challenges with EWOD devices are the deciding threshold voltage, used for clinical diagnostic to protect the cell from damage, avoiding the cross talk between electrodes because of electrostatic effect to maintain droplet on proper path and the automated multiplexing technique use for switching the electrode voltage.

In this thesis, the design parameters, voltage and switching time is obtained by trial and error method to maintain the shape and path of the droplet. This data is further used to simulate 2D and 3D mixing of dissimilar concentrated fluid.

Nomenclature

Symbol	Definition
μ	Dynamic viscosity
ρ	Density
γ_{SL}	Solid-liquid surface tension
γ_{LG}	Liquide-gas surface tension
γ_{SG}	Solid-gas surface tension
d	Dielectric layer thickens
U	Velocity scale
u	Vector velocity
p	Pressure
∇	Surface gradient operator
C	Capacitance
θ	Contact angle
n	Fluid concentration
M_f	Mesh flux
t	Time scale
D	Diffusivity
c	Diffusion constant

Contents

Declaration.....	iError! Bookmark not defined.
Approval Sheet	Error! Bookmark not defined.
Acknowledgements.....	iv
Abstract.....	v
Nomenclature	vi
Introduction	1
General	1
Literature review	3
Objective and Scope	5
Theory.....	7
Microfluidic biochips	7
Droplet actuation	7
The Principle of EWOD	8
Droplet Deformation	9
Droplet Transport	9
Modeling.....	10
Geometry (2-D & 3-D).....	11
Fluidic flow pattern and Boundary condition.....	13
Parameter and Meshing	15
Electrode Addressing.....	17
COMSOL Physics for simulation.....	22
Result and Discussion.....	22
Conclusion.....	38
References.....	39

Chapter 1

Introduction

General

Advancement in micro-fabrication processes has led the concept of Electrowetting on dielectric (EWOD), one of the ideal paradigm for lab-on-a-chip systems based upon micromanipulation of discrete droplets. It enables control over fluid shape and flow by electrical signals alone, which is viable by effective utilization of the excess charge accumulation at the interface between the droplet and the dielectric surface, also by polarization of line tension at the three-phase line.

EWOD helps in discretizing the flow and hence it is called as Digital microfluidic (DMF). DMF technology offers a platform for Lab-on-a-chip (LoC), which is concerned with the design of micro total analysis system (μ TAS) for chemical and biological applications with the advantages of portability, higher sensitivity, reagent volume reduction, faster analysis, increased automation, low power consumption, compatibility with mass manufacturing, and high throughput. This emerging technology combines electronics with biology to open new application areas such as point-of-care diagnosis, on-chip DNA analysis, and automated drug discovery.

Recent year a great deal of scientific research is being committed to automate, integrate and miniature microfluidic devices [1], [2], so that, it can be widely applicable and accessible. Various techniques such as thermocapillary [21] electrocapillarity [8] electro-osmosis [9], acoustics [10], electric forces [11], electromagnetic [12], electrophoresis [13], electrocapillary/electrowetting [22]–[25]) have been reported to advance the microfluidic devices, but among all EWOD is unique, because it is a direct way of controlling the surface tension of a fluid [17]. However Lab-on-chip (LoC) is such a device capable of handling a complete chemical or biological analysis protocol. One of the most prominent lines of research to attain this target consists in manipulating discrete volumes of fluids called droplets rather than forcing continuous phase flow, thus microfluidic based on electrowetting is often referred to as digital microfluidics [2]–[6].

It has been reported by Center for Drug Research that, “The development of new pharmaceuticals is extremely expensive and time consuming. It takes an average of 13 years and more than 1 billion USD to develop a new drug. The single biggest factor driving this cost is the rate of failure, which about 90% of drug discovery project failing in the late clinical phases of development” [14]. Also the Research in the field of chemistry, biology and medicine (clinical and

drug delivery) are lagging where the hundreds of reaction parallel need to take place simultaneously. These are the challenges that researchers are facing currently.

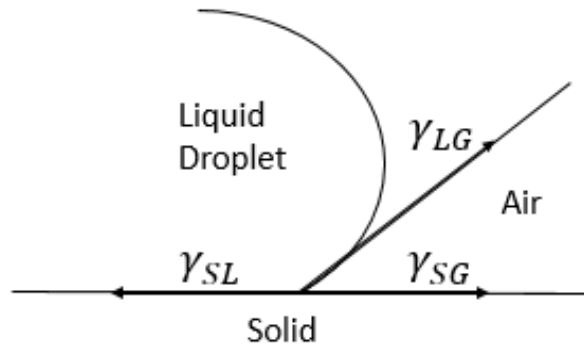


Figure 1: Three phase interphase line of solid, liquid and gas.....**Error! Bookmark not defined.**

The challenges with EWOD devices are the deciding threshold voltage, used for clinical diagnostic to protect the cell from damage [15], avoiding the cross talk between electrodes because of electrostatic effect to maintain droplet on proper track and the automated multiplexing technique use for switching the electrode voltage.

In this paper, we efforts to address the challenges with DMF system to enhance the system performance and also for transporting and merging application, using multiphase simulation modules of COMSOL Multiphysics. 2-D arrangement of all-in-single plane employed for simulation, resultant with ± 0.2 deviation of anticipated result.

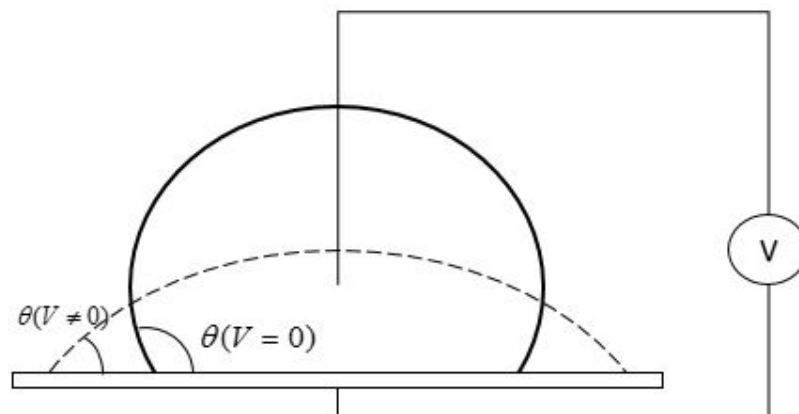


Figure 2: Electrowetting Principal. **Error! Bookmark not defined.**

Literature review

Shawn W. Walker, Benjamin Shapiro et al. (2009), work on the modeling and simulation of planar electrowetting on dielectric devices that move fluid droplets by modulating surface tension effects. They modeled fluid dynamic by Hele-Shaw type equation with a focus on inducing the relevant boundary phenomena. Also they include contact angle saturation and a contact line force threshold model that can account for hysteresis and pinning effects. Without them the simulations can predict droplet motion that is much faster than in experiments (up to 10-20 times faster). To handle surface tension, conservation of mass and the nonlinear contact line pinning in a straightforward and numerically robust way they present a variational method and a corresponding finite element discretization. Finally they compare the simulation data to available experimental data for different cases of droplet motion like splitting and joining. As a result they obtain

Moving glycerin droplet, the applied voltage (50V) switches between the left and right electrodes every 2 s. Each electrode is square with a side length of 1.5mm. The large time scale because glycerin is highly viscous.

Splitting water droplet, the three adjacent electrodes in a single row have the activation voltages of 25, 0 and 25V. Each electrode is approximately square with a side length of 1.4 mm.

Splitting glycerin droplet, the applied voltage (65V on the left and right electrodes) causes the droplet to be pulled apart and eventually split. Each electrode is approximately square with a side length of 1.5 mm. The relaxation time after pinchoff is 1100ms.

Joining water droplets, the applied voltage 65V on the center electrode only cause the two droplets to flow together and eventually merge. Each electrode is approximately square with a side length of 1.5 mm.

Tsung-Yu Ho, K. Chakrabarty et al. (2011) pointing the challenges facing biochips are similar to those faced by microelectronics some decade ago. To meet those challenges of increasing design complexity, they proposed computer-aided-design (CAD) tools for digital microfluidic biochip (DMFB). Their paper provides an overview of DMFBs and describes emerging CAD tools for the automated synthesis and optimization of DMFB designs, from fluidic-level synthesis and chip-level design to testing. With the assistance of CAD tools, user can concentrate on the development and abstraction of nanoscale bioassays while leaving chip optimization and implementation details to CAD tools.

D. Chatterjee, B. Hetayothin et al. (2006), reported for the first time that it is possible to manipulate droplets of organic solvents, ionic liquids, and aqueous surfactant solutions in air by these mechanisms using only modest voltages (<100 V) and frequencies (<10 kHz). The feasibility of moving any liquid can be predicted empirically from its frequency-dependent complex permittivity, ϵ^* . The threshold for droplet actuation in air with our two-plate device configuration is $|\epsilon^*| > 8.6 \times 10^{21}$.

Yen-Chen Lin, Kai-Cheng Chuang et al. (2006), are investigated on EWOD (electrowetting-on-dielectric) and LDEP (liquid dielectrophoresis) to provide digital and analog microfluidic functions on an integrated chip respectively. They succeed to integrate EWOD and LDEP on a single chip. EWOD is the driving mechanism for droplets in digital microfluidics. To provide sufficient voltage without electrolysis, 1 kHz signal was desirable for EWOD. EWOD actuation with different frequency, dielectric and surrounding media were tested. At 100 kHz, the EWOD actuation is less effective since the voltage across the dielectric is reduced. Moreover at 100 kHz, the expelling of satellite droplets was found. LDEP was found when manipulate liquid droplet in oil by applying 100 kHz. Three fundamental tools of integrated digital and analog microfluidics were developed in this paper, including a digital-to-analog microfluidic converter, an analog to digital microfluidic converter, and a valve.

Hyejin Moon and Sung Kwon Cho (2002), discusses and experimentally verifies how to lower the operating voltage that drives liquid droplets by the principle of electrowetting on dielectric (EWOD). Typically, much higher voltages (>100 V) are used to change the wettability of an electrolyte droplet on a dielectric layer compared with a conductive layer. Using very thin (700 Å) and high dielectric constant (~180) materials, they achieved a significant contact angle change (120° to 80°) has been achieved with voltages as low as 15 V. A contact angle change of (120° to 80°) could be obtained at about 25 V for the SiO₂ films. A high dielectric constant material can reduce the EWOD voltage even further. By incorporating BST (=180) as the main insulation layer, they succeeded in obtaining a contact angle change of (120° to 80°) with only 15 V. To demonstrate the utility of this result, they applied the findings to the microfluidic device, successfully driving nanoliter-scale water droplets in a microchannel with only 15 V.

Roland Baviere, Jerome Boutet, et al. (2008), reports on the dynamics of droplets in the capillary regime induced by electrowetting-on-dielectric actuation. They used side-view observations of stroboscopic recording techniques to measure and analyse droplet deformations as well as the front and rear apparent contact angles during motion. Secondly, the influence of

viscosity on the droplet velocity as a function of the applied voltage was studied. Finally, the influence of the dielectric thickness on the droplet dynamics was studied. They studied Influence of viscosity on the velocity variation as a function of actuation voltage, for water/glycerol mixtures.

Real apparent contact angle measured at the transition between phages.

Comparison for water droplet between apparent static and dynamic contact angles.

Comparison of experimental data with Brochard's model (numerical parameters in the text)

Comparison between static and dynamic electrowetting for a water droplet

Effect of dielectric and hydrophobic layer thickness on the velocity variation of a water droplet as a function of actuation voltage

Liguo Chen, Xiawei Xu, et al. (2013), demanded the root reason for EWOD is the instantaneous pressure difference inside a droplet, which was obtained by means of numerical simulation. First, based upon the theory of EWOD, they design a graphical model of EWOD using VOF method. Next, driving that two kind of fluid which should follow the law of mass conservation and principle of momentum conservation. They conclude, In one period of motion, the highest pressure region inside a droplet will keep changing and transferring along with the driving time until a steady state of pressure difference is obtained, beside the much longer driving time is, the much larger pressure difference will be inside a droplet.

Objective and Scope

- Based on the literature review, importance and challenges the objective of the project are
- Change in droplet shape or contact angle by applying the electrical voltage to the dielectric coated electrode.
- Analysis of voltage distribution in EWOD system. To study the capacitance effect and velocity profile of droplets.
- Moving the droplet from one electrodes to others by switching the voltage from current electrode to adjacent electrode.
- Designing 2-d and 3×3 array of electrodes platform for simulation.

- Mixing two droplets having dissimilar concentration.
- Selecting the suitable design parameter, material and methodology, so that the threshold voltage would be as minimum as possible to protect cells from damage.
- Avoiding the cross talk between electrodes to maintained droplets over proper track.
- Efficient switching addressing of the electrodes for multiplexing large number of switch by having less number of input pin

The Scope of this project are

- Can be fabricated using micro/nano fabrication technology.
- Droplets can split, can be created by integrating reservoir with microfluidic platform.
- Numerous chemical and biological experiment can perform on the same platform.

Chapter 2

Theory

Microfluidic biochips

For conventional biochemical laboratories microfluidic biochips or lab-on-a-chip are the better platform. It have revolutionizing many application, such as DNA analysis, proteomics, clinical pathology, and molecular biology procedures. There are two type of biochips, microarray and microfluidic biochip. Microarray is again classified as DNA array and Protein array. Whereas microfluidic biochip are of continuous type and discrete type microfluidic. The continuous type flow can be carried out by using permanently etched channel, micro pump, micro valves and micro channels. On the other hand discrete type or digital microfluidic have all the control parameter in electrical domain, no mechanical component involvement in the process. Also each droplets controlled independently over the $m \times n$ array of electrodes. The advantages of discrete type flow over continuous flow are reusability, re-configurability and electrical domain parameters. The challenges facing biochips are similar to those faced by microelectronics some decades ago. A typical microprocessor today has over a billion transistors. Such a design complexity is possible because engineers are using Computer-Aided Design (CAD) tools, which, starting from a specification of the desired functionality, automatically build the best possible design (such a process is called top-down design). As in the microelectronics area, comsol tools will reduce the development costs, increase the design productivity and yield, and are the key to the further growth and market penetration of biochips. My research vision is to develop a design flow for biochips, which, starting from a system specification can automatically derive a physical biochip design.

Droplet actuation

There are several techniques that have been proposed for actuating the droplet like Electric forces, Electromagnetic, Electrocapillarity, Electro-osmosis,

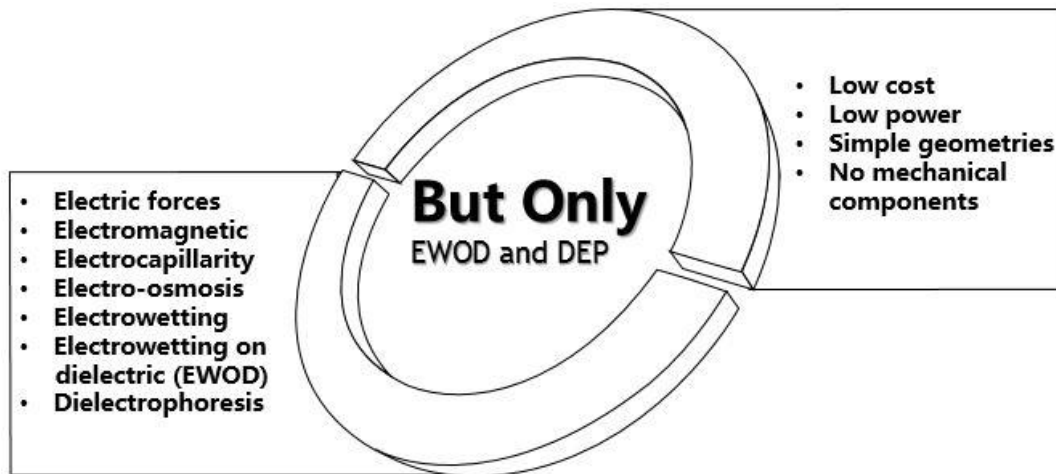


Figure 3: Available techniques and their advantages **Error! Bookmark not defined.**

Electrowetting, Electrowetting on dielectric (EWOD) and Dielectrophoresis (DEP) but among all the EWOD is unique, because of Low cost, Low power, Simple geometries and No mechanical components. The electrical methods for droplet actuation are DEP and EWOD. DEP uses High frequency ac & high amplitude voltages ac voltage of 230-300Vrms at 50-200 kHz. Whereas EWOD uses Low frequency (<1 kHz) Low amplitude of DC voltages. The advantages of EWOD over DEP are almost negligible Joule heating effect, direct way of controlling the surface tension Helping the multiple droplets to act like small micro reactors.

The Principle of EWOD

Lippmann proposed that by applying external voltage across the capillary, an electrostatic field will be generated and because of electrostatic charge interfacial tension between liquid-gas and liquid-substrate will change [16], eventually resulting in deformation of a liquid droplet (Figure 2), This phenomenon of droplet deformation due to change in contact angle effected by applied voltage is referred to as electrowetting on dielectric (EWOD). Because of applied voltage two phenomenon may occurs, one is droplet will change its shape and deform if the voltage applied to the same electrode, or else droplet will deform at the same time will move to adjacent electrodes if applied voltage is to the next or adjacent electrode. Because of electric voltage there will be electric field, and there is chance that droplet will undergo to electrolysis if the applied voltage is high. So to protect the droplet from electrolysis the dielectric layer is used on the top of the electrodes so that the electric field will be less

and joule heating effect. Also the top of the microfluidic platform need to be hydrophobic to sustain the droplet shape.

Droplet Deformation

When a potential is applied, an electric field will generate (because of excess charge accumulation at three phase line tension [14]-[17], [25] or polarization of dielectric layer [7]), which lead the change in interfacial tension or surface tension between the liquid-gas and liquid-solid, resulting as change in contact angle or droplet deformation. The solid-liquid interfacial tension (γ_{SL}) (Figure 1) can be controlled by the electrical potential across the interface, and the result is expressed by using the Lippmann's Eq. (1) [16]

$$\gamma_{SL}(V) = \gamma_{SL}(0) - \frac{1}{2} CV^2$$

Where C (F/m²) is the capacitance of the dielectric layer, V is the applied voltage and $\gamma_{SL}(0)$ is the solid-liquid interfacial tension at potential zero.

The contact angle (θ) of droplet at the interface of dielectric layer can be measure by Young's Eq. (2) [19]

$$\cos\theta = (\gamma_{SG} - \gamma_{SL}) / \gamma_{LG}$$

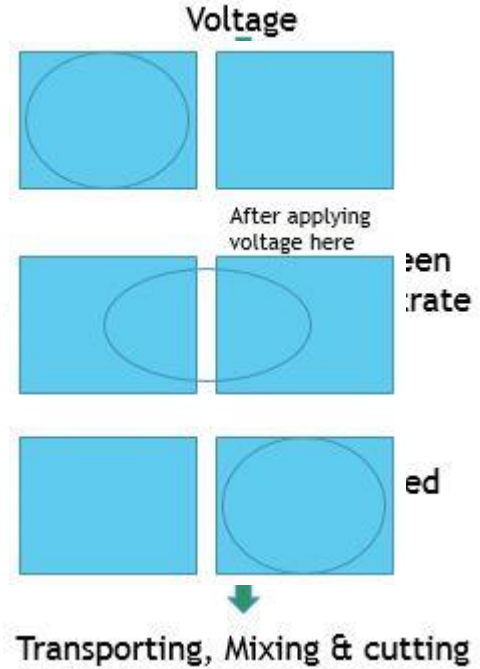
Where γ_{SG} and γ_{SL} are the interfacial tension of solid-gas and liquid-gas respectively. Incorporating the Young's Eq. to the Lippmann's Eq. (3), the resulting the change in contact angle $\theta(V)$ due to applied potential (V), and hence called Lippmann-Young equation

$$\cos\theta(V) = \cos\theta(0) + \frac{\epsilon_0\epsilon}{2\gamma_{LG}d} V^2$$

Here, $\theta(V)$ is the resting contact angle i.e. without any applied potential. ϵ (8.85×10^{-12} F/m) is the permittivity of the free space, ϵ is the dielectric constant of dielectric layer, and d is the thickness of the dielectric film. Note that γ_{SG} and γ_{LG} assumed to be constant i.e. independent of applied potential [20].

Droplet Transport

A droplet can be transported by switching the voltage from current electrode to adjacent electrode, this cause asymmetrical change in the three phase line



tension. No matter which method use for changing the interfacial tension (e.g., Electrocapillarity [8] Electro-osmosis [9], Acoustics [10], Electric forces [11], Electromagnetic [12], Electrophoresis [13] Thermocapillary [21] or Electrocapillary/Electrowetting[22]–[25]), the asymmetrical change in the interfacial tension induces an asymmetrical deformation of the liquid meniscus, which establishes a pressure difference inside liquid, gives a bulk fluid movement [26], which can be predicts using Brochard’s model Eq. (4) [22], [27].

$$U = \frac{\varepsilon_0 \varepsilon (1 - \cos \theta(V))}{6 \mu l \sin \theta(V)} V^2$$

Where μ and l are the viscosity of the droplet and an empirical factor respectively.

Chapter 3

Modeling

The modeling of geometry is of two type 2-D and 3-D. Firstly we designed the 2-D geometry of single droplet on the single electrode platform to calculate and find out the suitable design parameters. Then we continue the same with droplet packet transformation on a single droplet on single line planer four

electrodes. Finally we integrated the concept with convection diffusion equation to mix two droplets having different concentration. The study continued for 3-D simulation.

In this section, we discuss geometry design, Fluidic flow pattern and Boundary condition, COMSOL Physics used for simulation and electrode addressing.

Geometry (2-D & 3-D)

The principal of various fluidic-operation is droplet manipulation. Although various geometry with driving factor has been proposed [28], [29]. The EWOD chips have much more attention because of portability, higher sensitivity, reagent volume reduction, faster analysis, increased automation, low power consumption, compatibility with mass manufacturing, and high throughput [25], [30] and also for direct way of controlling the surface tension of a fluid [17]. Figure 4(left) is used for performing the Lippmann-Young equation principal i.e. change in contact angel. The Brochard’s model has been implemented on Figure 4(right). The critical and suitable geometry parameter has been derived using both the Figure 4(right and left). Figure 5(right) represent the schematic view of the EWOD platform. ‘T’ shape platform (Figure 5(left)) is designed for testing and simulation of droplet transport and mixing. The simulation for change in contact angle has been carried out on Figure 4(left) platform whereas Figure 4(right) geometry has used for finding the saturation voltage. Figure 6 use for 3-D simulation of change in contact angle. The 3-D packet transform has been perform on figure 7. Finally figure 8 is used for 3-D mixing. The principle of Lippmann-Young equation and Brochard’s model has been implemented to deformation and transportation respectively. The width and length of the electrodes are $5\mu\text{m}$ and $5.5\mu\text{m}$ respectively for 1-6 electrodes, for 8-11 electrodes it is $6.7\mu\text{m}$ and $7\mu\text{m}$ respectively and for 7 it is $5\mu\text{m}$ and $7\mu\text{m}$ respectively. The different size of electrodes are chosen as the fluid volume is different at different time and places. The 3-D shape of the droplet obtain by revolving 360° of half 2-D droplet.

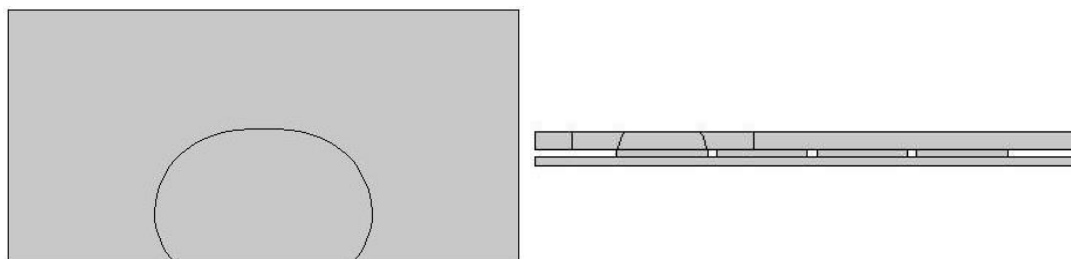


Figure 4: 2-D geometry for contact angle simulation and droplet packet transform
 **Error! Bookmark not defined.**

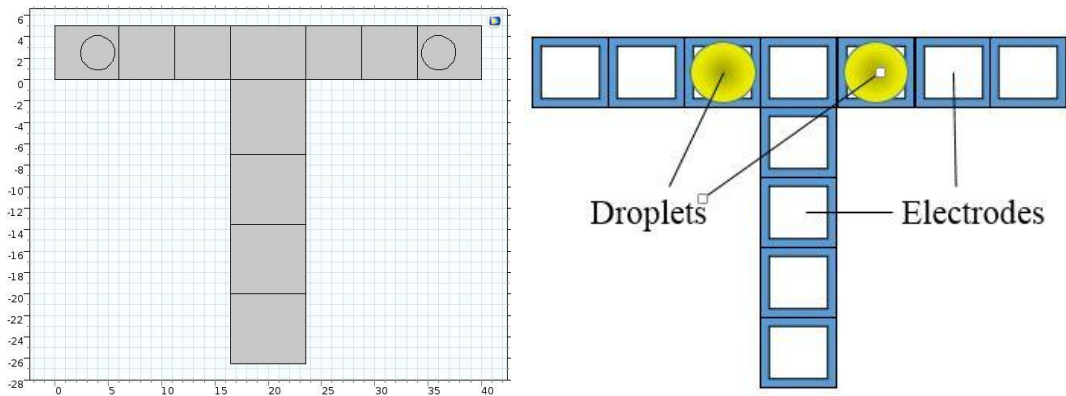


Figure 5: 2-D geometry for mixing application..... **Error! Bookmark not defined.**

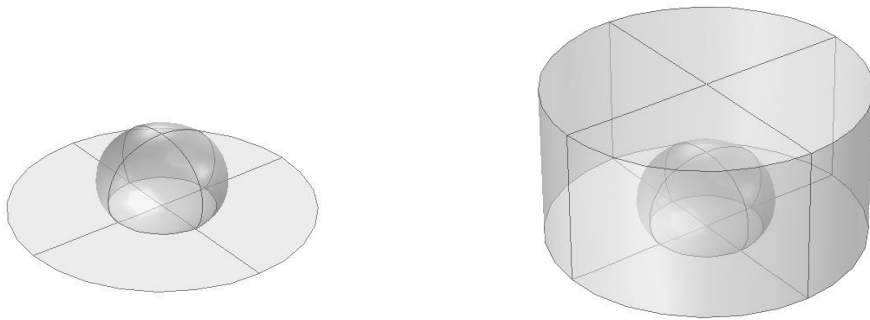
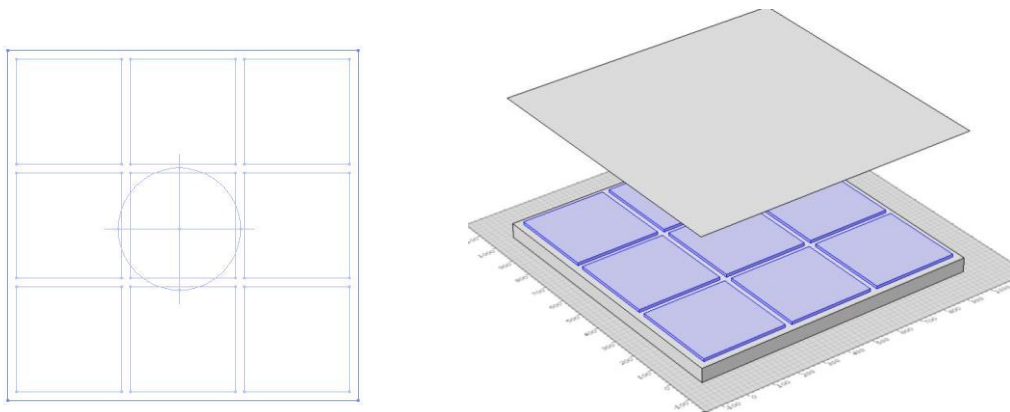


Figure 6: 3-D geometry for change in contact angle..... **Error! Bookmark not defined.**



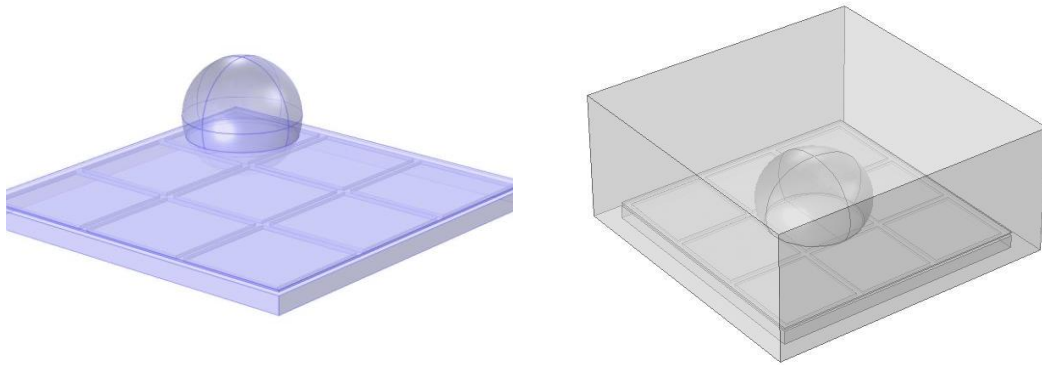


Figure 7: 3-D geometry for droplet packet transform.....**Error! Bookmark not defined.**

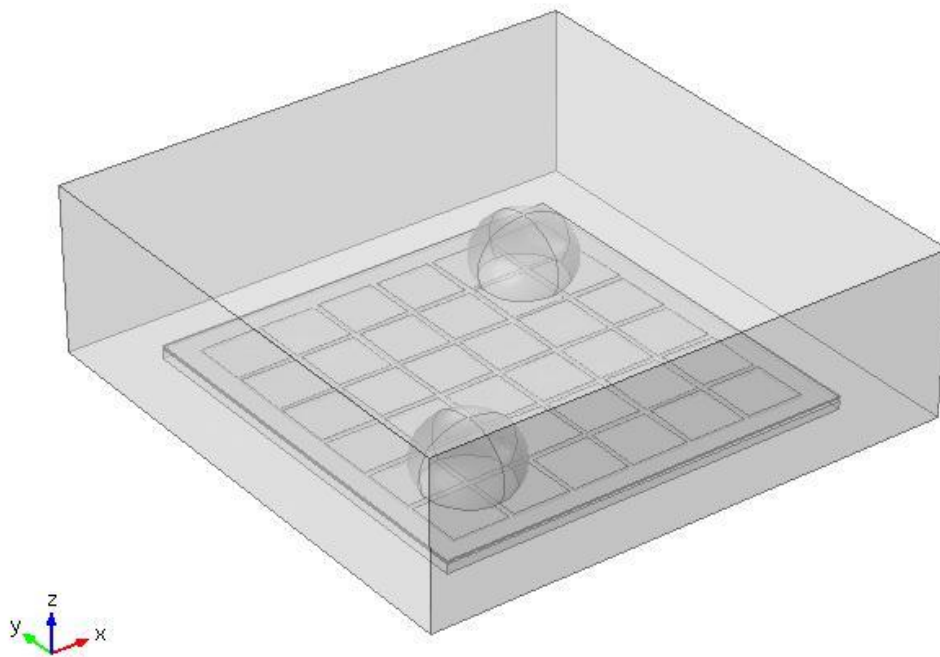


Figure 8: 3-D geometry for droplet transform and mixing application**Error! Bookmark not defined.**

Fluidic flow pattern and Boundary condition

Assuming fluid flow as Incompressible flow and also neglecting the inertial term (stokes flow), the Navier–Stokes equation can be expressed as Eq. 5 where, U is the fluid velocity, ρ is the fluid density, p is the pressure, μ is the dynamic viscosity, F is the represents body forces per unit volume and ∇ is the vector operator

$$\rho \frac{\partial U}{\partial t} + \rho(U \cdot \nabla)U = -\nabla p + \mu \nabla^2 U + F$$

$$\nabla \cdot U = 0 \quad (5)$$

Convection Diffusion equation has been used for mixing two different concentrated fluid. The droplets have the concentration 0 and 1 mol/m³ respectively.

$$d_a \frac{\partial con}{\partial t} + \nabla \cdot (-c \nabla con) + \beta \cdot \nabla con = f$$

$$\nabla = \left[\frac{\partial}{\partial x}, \frac{\partial}{\partial y} \right] \quad (6)$$

Where d_a is the damping coefficient, β is the convection coefficient, c is the diffusion coefficient, and con is the concentration, f is the source term. All the values of coefficient are one.

The liquid-air interface can be defined for time dependent solution as Eq. (7)

$$u_1 = u_2 \cdot n_1 \cdot T_1 = \sigma (\nabla_t \cdot n_1) n_1 - \nabla_t \sigma$$

$$u_1 = u_2 + M_f \left(\frac{1}{\rho_1} + \frac{1}{\rho_2} \right) n_1 \quad (7)$$

$$u_{mesh} = (u_1 \cdot n_1) - \frac{M_f}{\rho_1} n_1$$

Where ρ_1 and ρ_2 are the density of the fluid and air. u_1 and u_2 are the velocity of fluid and surrounding air respectively. n_1 and n_2 are the concentration of respective fluids. M_f is the mass flux, which we chosen zero, then the Eq 7 can be simplified as

$$u_1 = u_2$$

$$u_{mesh} = (u_1 \cdot n_1)$$

The fluid and dielectric interface defined as $\theta_c = \theta_w$, where θ_w is represented in Eq. 3

The Navier–Stokes equation is used for calculating surface velocity profile of the droplet, then that velocity coupled with level set method and convection diffusion equation for transporting the droplet with deformation and mixing

application. The level method expression for time dependent and incompressible fluid is as follows.

$$\rho \frac{\partial u}{\partial t} + \rho(u \cdot \nabla)u = \nabla \cdot [-pl + \mu(\nabla u + (\nabla u)^T)] + f$$

$$\nabla \cdot u = 0$$

Parameter and Meshing

The droplet is chosen as water droplet having the dynamic viscosity of 1.002 Pa-s. The electrodes material chosen as copper and top hydrophobic material as ITO. The meshing element, grid and degree of freedom is different for different geometry. The geometry of single electrodes change in contact angle have the total number of meshing element are 15657 and edge element are 671. The packet transform geometry has total number of element 27601. The 3-D geometry of change in contact angle of 43962 element. Whereas for packet transform of 3-D geometry has 455181 element. The 2-D convection diffusion mixing geometry have the total number of meshing element of 67526. The selective meshing has been done for all geometry. The selective meshing have the certain advent of less number of meshing element will be less, less simulation time, good resolution and good contrast etc.

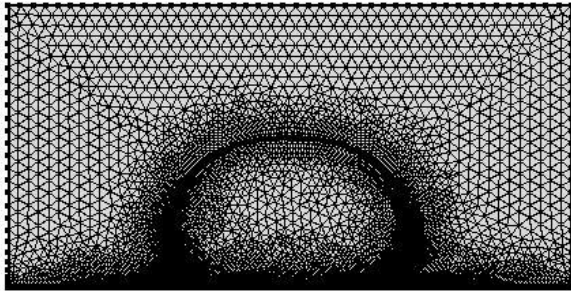


Figure 9: 2-D meshing for change in contact angle **Error! Bookmark not defined.**



Figure 10: 2-D meshing for droplet packet transform..... **Error! Bookmark not defined.**

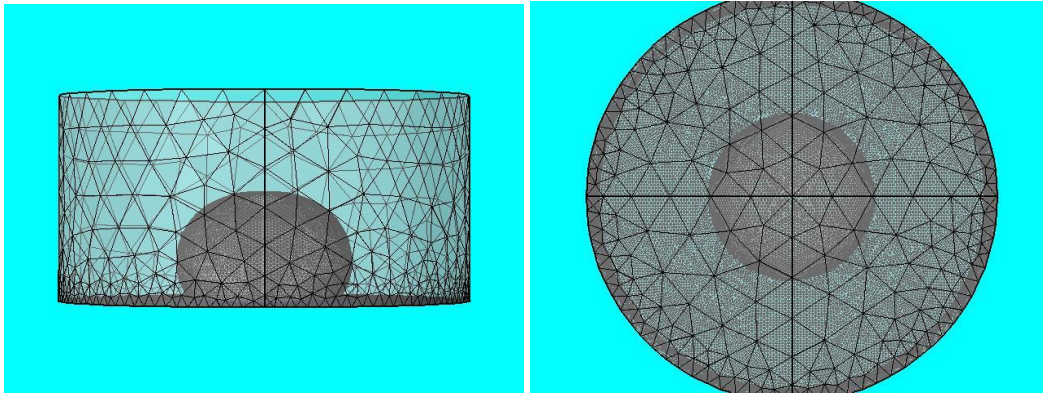


Figure 11: 3-D meshing for change in contact angle **Error! Bookmark not defined.**

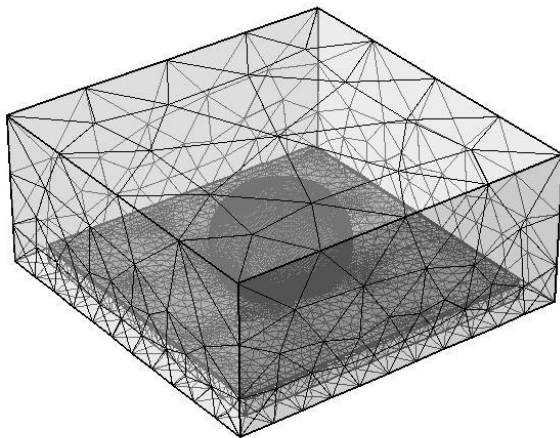
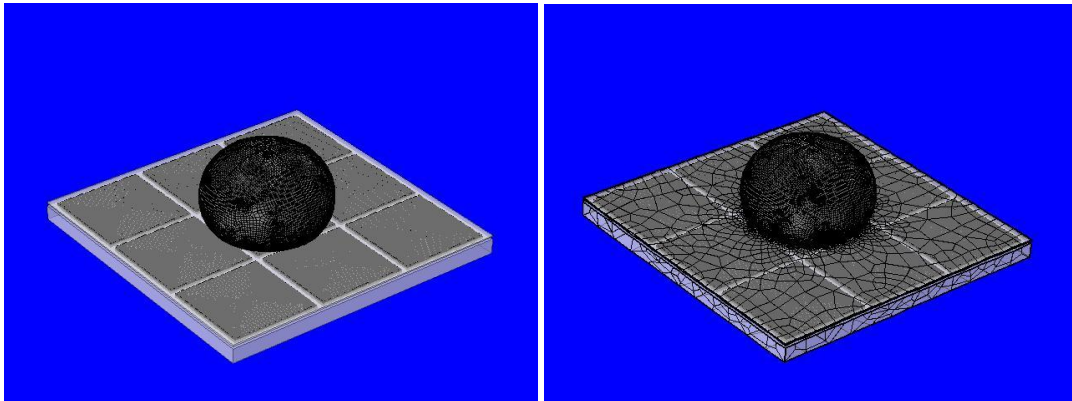


Figure 12: 3-D meshing for droplet packet transform **Error! Bookmark not defined.**

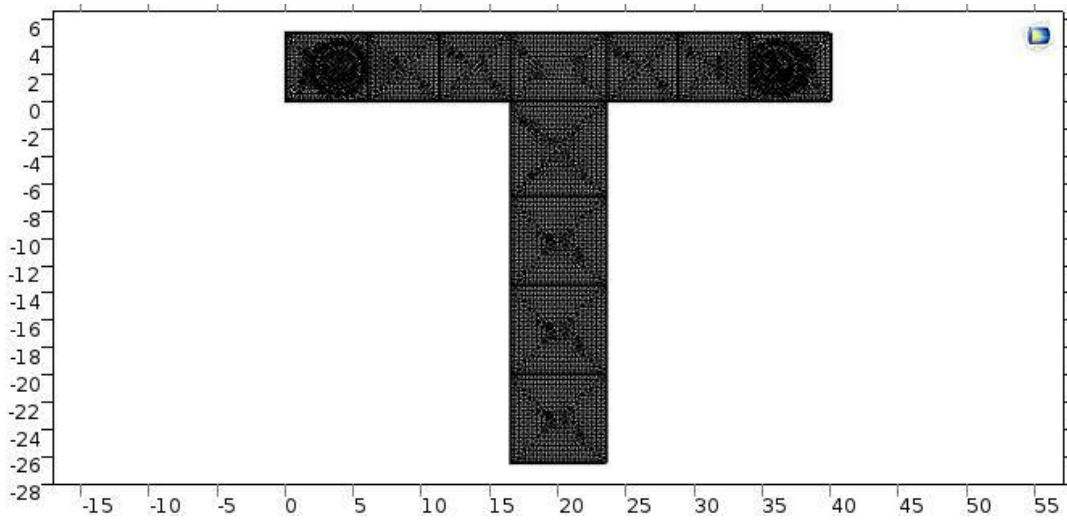


Figure 13: 2-D meshing for mixing application **Error! Bookmark not defined.**

Electrode Addressing

It is a method to apply and switch the potential from current electrode to adjacent electrode. The efficient switching mechanism is required for mixing number of fluids. The efficient mixing can be possible by varying the space and time parameter. The Lippmann-Young Eq. can be simulated only by applying and removing potential from the same electrode with respect to time parameter [32], whereas droplet transport and mixing has been simulated by switching the potential from current electrode to adjacent electrode with respect to space and time parameter (Figure 14). The time delay for switching and the electrodes activation time is very crucial parameter for application such as mixing and transport. The matlab interphase is coupled with comsol for switching the electrode voltage. Each and every electrode is allocated with specific parameter. Those parameter are called for activation and deactivation of the electrodes. The activation time is 0 Sec and delay/pause time is 0.07 Sec. By various testing and simulation we have obtained the effective delay of 0.07 s.

Table 1: Electrode addressing

Electrodes	1	2	3	4	5	6	7	8	9	10	11
	1	1	0	0	×	×	×	×	×	×	×
	0	0	1	1	0	0	×	×	×	×	×
Activation	×	×	0	0	1	1	0	0	×	×	×

Sequence	x	x	x	x	x	0	1	0	x	x	x
	x	x	x	x	x	x	0	1	0	x	x
	x	x	x	x	x	x	x	0	1	0	x
	x	x	x	x	x	x	x	x	0	1	0
	x	x	x	x	x	x	x	x	x	0	1

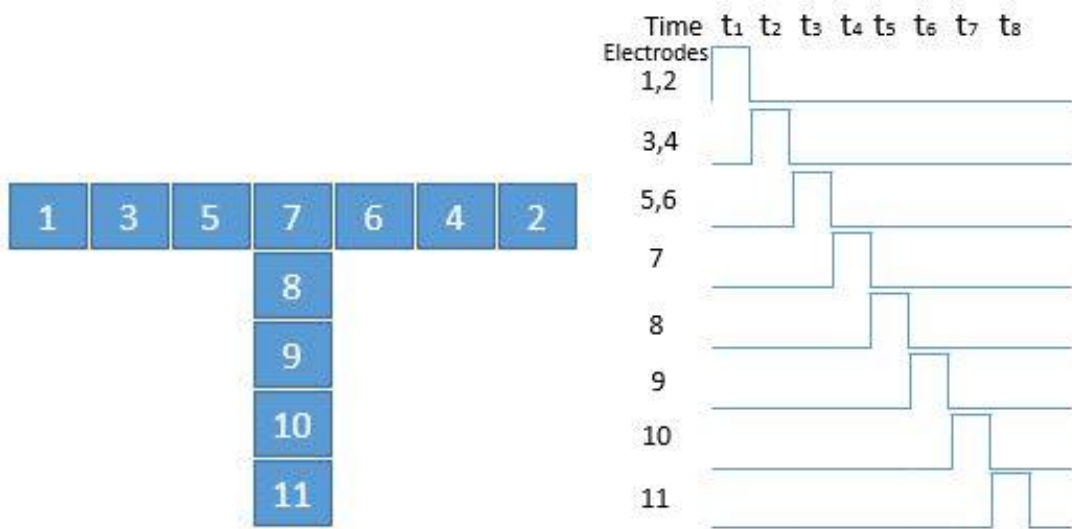


Figure 14: Diagrammatic view of electrodes switching..... **Error! Bookmark not defined.**

Matlab code for electrode Switching

```

%-- connect to the COMSOL
a = function retval ('COM5.0')

%-- specify pin mode
a.pinMode(1-10,'input');
a.pinMode(11,'output');

%-- digital i/o
Elec1 = '1,2';

```

```
switch(elec1)
a.digitalRead(1,2) % read pin 1,2
a.digitalWrite(13,0) % write 0 to pin 13
case 'A'
```

```
Activate (1,2)
```

```
Deactivate (3,4)
```

```
Fprintf (1 & 2 are activated);
```

```
Pause(0.07) %in seconds
```

```
Elec2 = '1,2';
```

```
switch(elec2)
a.digitalRead(3,4) % read pin 3,4
a.digitalWrite(13,0) % write 0 to pin 13
case 'A'
```

```
Activate (3,4)
```

```
Deactivate (1,2,5,6)
```

```
Fprintf (3 & 4 are activated);
```

```
Pause(0.07) %in seconds
```

```
Elec3 = '5,6';
```

```
switch(elec3)
a.digitalRead(5,6) % read pin 5,6
a.digitalWrite(13,0) % write 0 to pin 13
case 'A'
```

```
Activate (5,6)
```

```
Deactivate (3,4,7)
```

```
Fprintf (5 & 6 are activated);
```

```
Pause(0.07) %in seconds
```

```
Elec4 = '7';
```

```
switch(elec4)
a.digitalRead(7) % read pin 7
```

```
a.digitalWrite(11,0) % write 0 to pin 11  
case 'A'
```

```
Activate (7)
```

```
Deactivate (5,6,8)
```

```
Fprintf (7 are activated);
```

```
Pause(0.07) %in seconds
```

```
Elec4 = '7';
```

```
switch(elec4)
```

```
a.digitalRead(7) % read pin 7
```

```
a.digitalWrite(11,0) % write 0 to pin 11  
case 'A'
```

```
Activate (7)
```

```
Deactivate (5,6,8)
```

```
Fprintf (7 are activated);
```

```
Pause(0.07) %in seconds
```

```
Elec5 = '8';
```

```
switch(elec5)
```

```
a.digitalRead(8) % read pin 8
```

```
a.digitalWrite(13,0) % write 0 to pin 13  
case 'A'
```

```
Activate (8)
```

```
Deactivate (7,9)
```

```
Fprintf (8 are activated);
```

```
Pause(0.07) %in seconds
```

```
Elec6 = '9';
```

```
switch(elec6)
```

```
a.digitalRead(9) % read pin 9
```

```
a.digitalWrite(11,0) % write 0 to pin 11  
case 'A'
```

```
Activate (9)
```

```
Deactivate (8,10)
Fprintf (9 are activated);
Pause(0.07) %in seconds
```

```
Elec7 = '10';
switch(elec7)
a.digitalRead(10) % read pin 10
a.digitalWrite(11,0) % write 0 to pin 11
case 'A'
Activate (10)
Deactivate (9,11)
Fprintf (10 are activated);
Pause(0.07) %in seconds
```

```
Elec8 = '11';
switch(elec8)
a.digitalRead(11) % read pin 11
a.digitalWrite(11,0) % write 0 to pin 11
case 'A'
Activate (11)
Deactivate (10)
Fprintf (11 are activated);
Pause(0.07) %in seconds
```

```
%-- close session
delete(a)
```

The total switching time is of 0.49 Sec for mixing two fluid. While activating some electrode the adjacent electrodes must be deactivated and are in don't care condition.

COMSOL Physics for simulation

AC/DC, Fluid Flow and Chemical Species Transport physics are used for simulation in COMSOL platform. In particular we use Electric Current (ec), Laminar Two-Phase Flow, Moving Mesh (tpfmm) for simulation of Lippmann-Young equation i.e change in contact angle for droplet deformation, additionally Level Set (tpf) with Electric Current (ec) for simulation of 2D droplet transport and Convection-Diffusion Equation (cdeq) for mixing two different concentrated droplets. This physics are used for both 2-D and 3-D. The surface velocity is calculated by Laminar Two-Phase Flow, Moving Mesh (tpfmm) using navier stokes equation then that coupled with level set method and convection diffusion equation for transporting and mixing droplets respectively.

Chapter 4

Result and Discussion

The change in contact angle and transportation of a single droplet has been simulated to find the proper set of design parameter and the voltage criteria. It has been studied that the critical voltage is of 12.7 V whereas the saturation voltage is 17.5 V. Also we studied for other intermediate voltages. Above 17.5 V the droplet shape is getting distorted. Element size scale factor for meshing the simulation of Lippmann-Young equation was chosen as 0.2, whereas the scale factor chosen for the study of droplet transport was 0.5. Navier Slip boundary condition was implemented to represent the liquid-solid interface for both the cases of simulation. The prescribed mesh displacement property applied to the

left and right boundary for the simulation of Lippmann-Young equation.

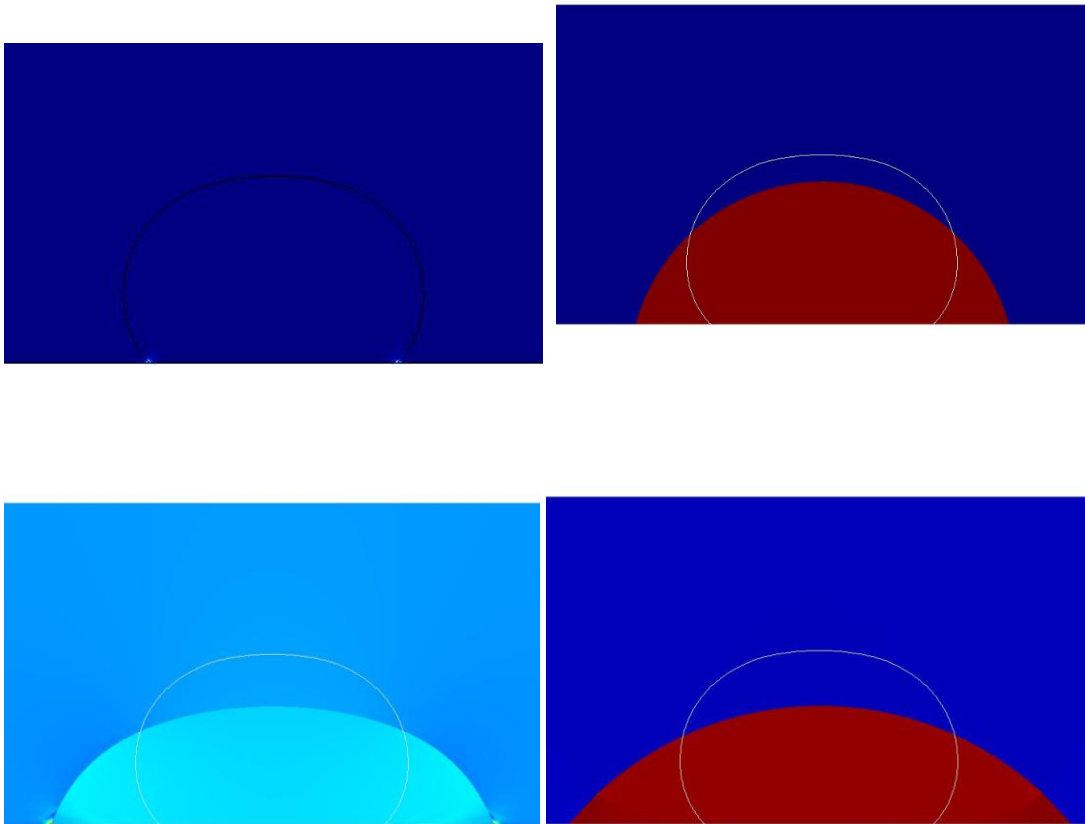
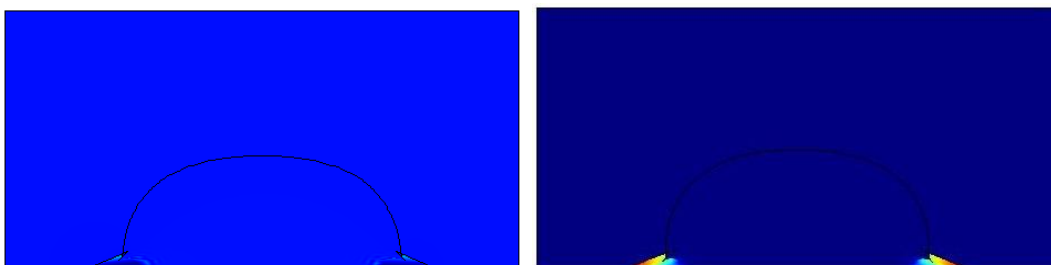


Figure 15: Contact angle with respect to 0, 12.7, 15 and 17.5 V respectively..**Error! Bookmark not defined.**

The below rembo colors indicating the electric field distribution across the fluid. Result shows effective change in contact angle taken place from 12.7 V to 17.5 V, behind the 17.5 V there is no change in the droplet shape i.e. saturated but because of high electric voltage stronger electric field distribution.



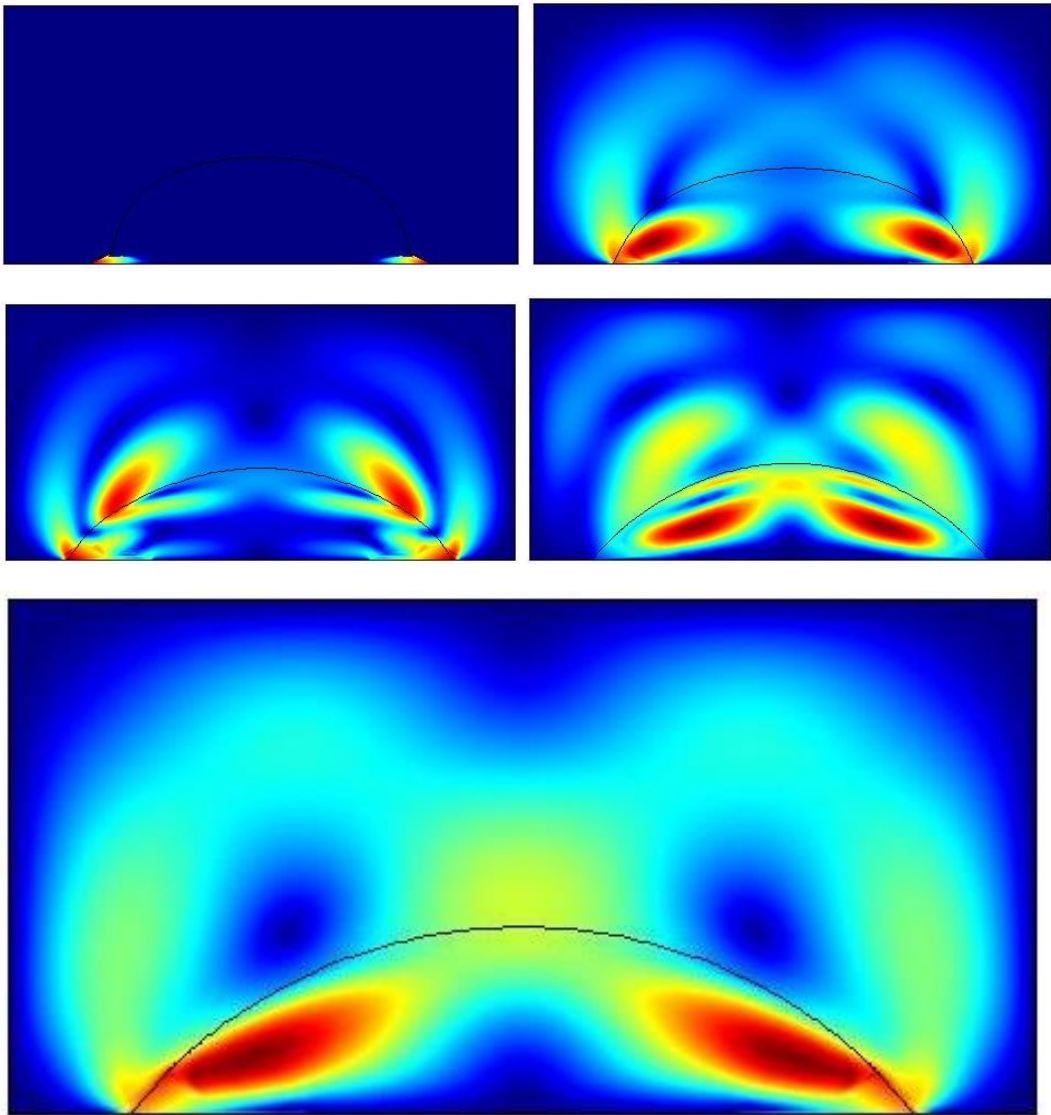


Figure 16: Electric field simulation. The droplet is getting saturated but still there is a change in electric field..... **Error! Bookmark not defined.**

To maintain the shape of the droplet another simulation has been performed, where it studied that above certain voltage no more shape deformation, but if the voltage farther increase beyond certain value then shape of the droplet will get distorted. The saturation voltage is same as the 2-D contact angle simulation i.e. 17.5 V, but the maximum limit is of 22 V.



Figure 17: Droplet shape is getting distorted behind 22 V ... **Error! Bookmark not defined.**

The change in contact angle with respect to 0, 12.7, 15 and 17.5 V is shown in figure 15. The study has been continued for 14.9 V and 15.3 V. The change in contact angle and the relative change in contact angle has been recorded and listed on below table.

Table 2: Relative Change in Contact angle with respect to voltages.

Voltage (V)	Contact angle (θ)	Relative Change in contact angle (θ)
0	130°	0°
12.7	126°	4°
14.3	114°	10°
15.9	90°	24°
17.5	51°	39

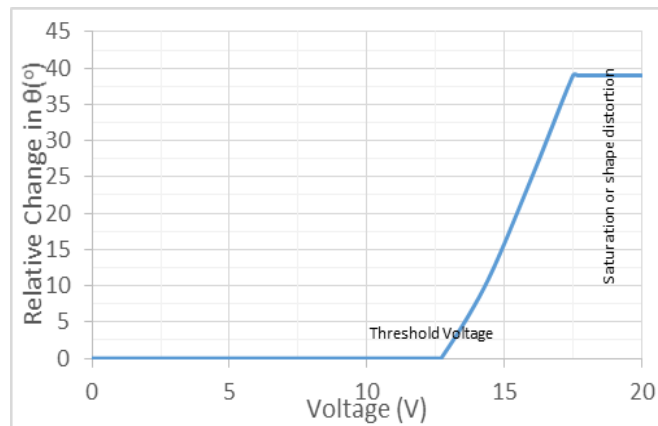


Figure 18: Contact angle modulation efficiency plot **Error! Bookmark not defined.**

The graph is showing the relative change in contact angle Vs voltage. Operating voltage must lie on the slope line.

An arrangement containing four electrodes in line. The simulation results on single droplet transport and switching at different time in below Figure 19 (a), (b), (c), (d), (e), (f), (g) and (h) respectively by applying wide range of voltage. Droplet packet transform has been simulated and the switching delay time is 0.002 Sec. The experiment has been done for forward and reverse transform.

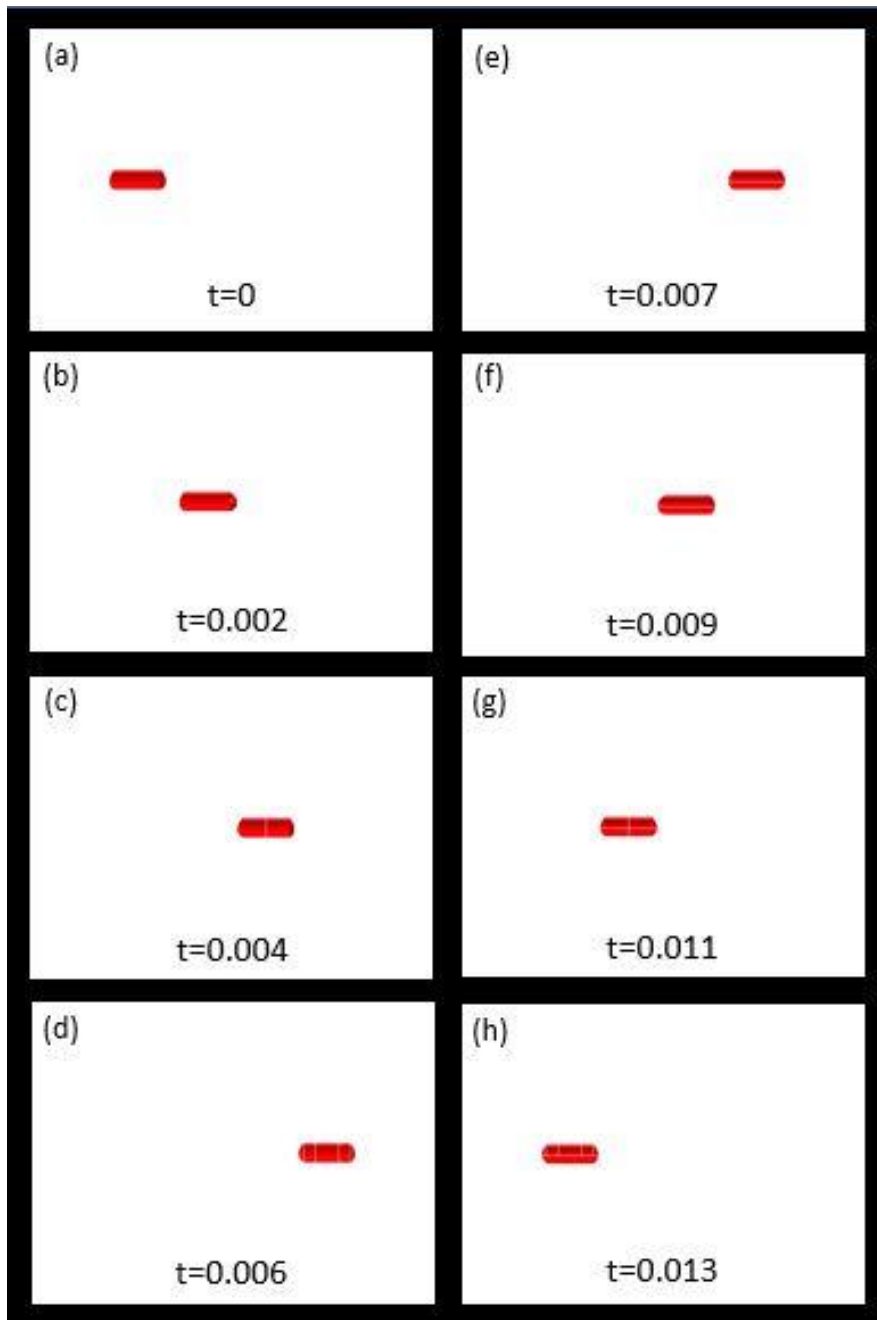


Figure 19: (a), (b), (c) and (d) are the position of the droplet when the compounding electrode voltage is 15V and others are at 0V.

3-D droplet simulation for change in contact angel has been experimentally done on single electrodes, where the variables are in time domain. The applied voltages are of 13 V, 15 V and 19 V respectively.

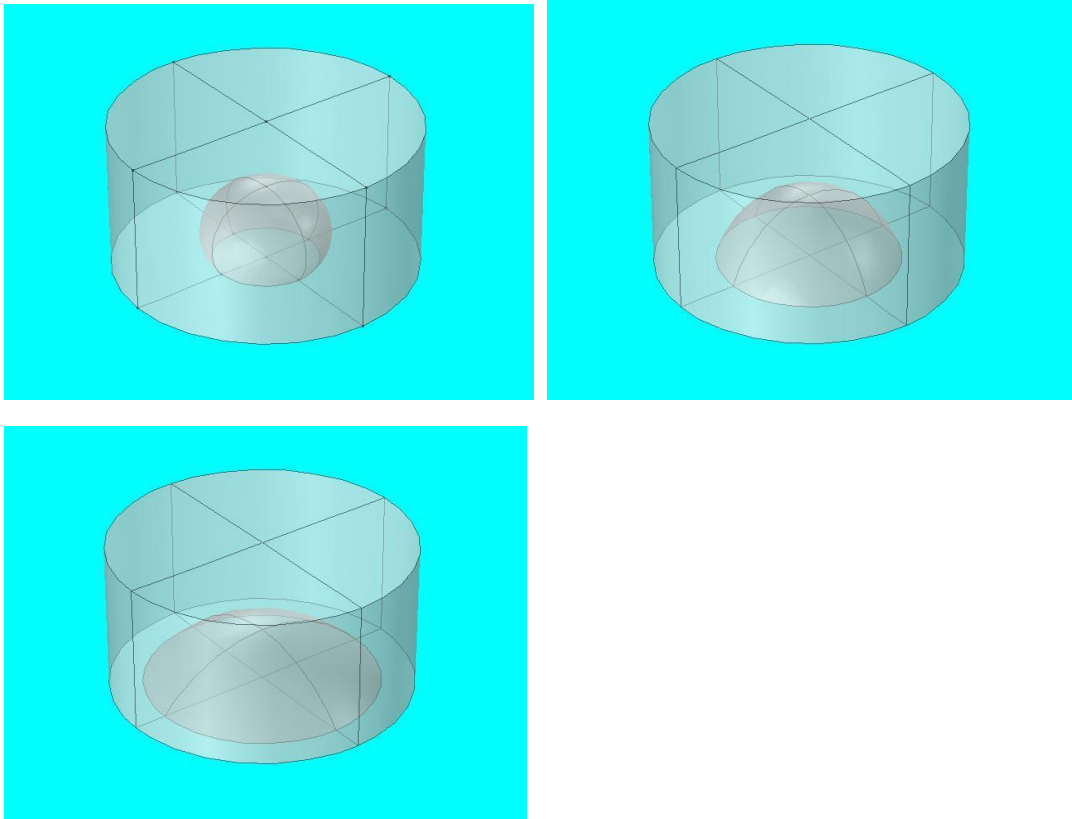
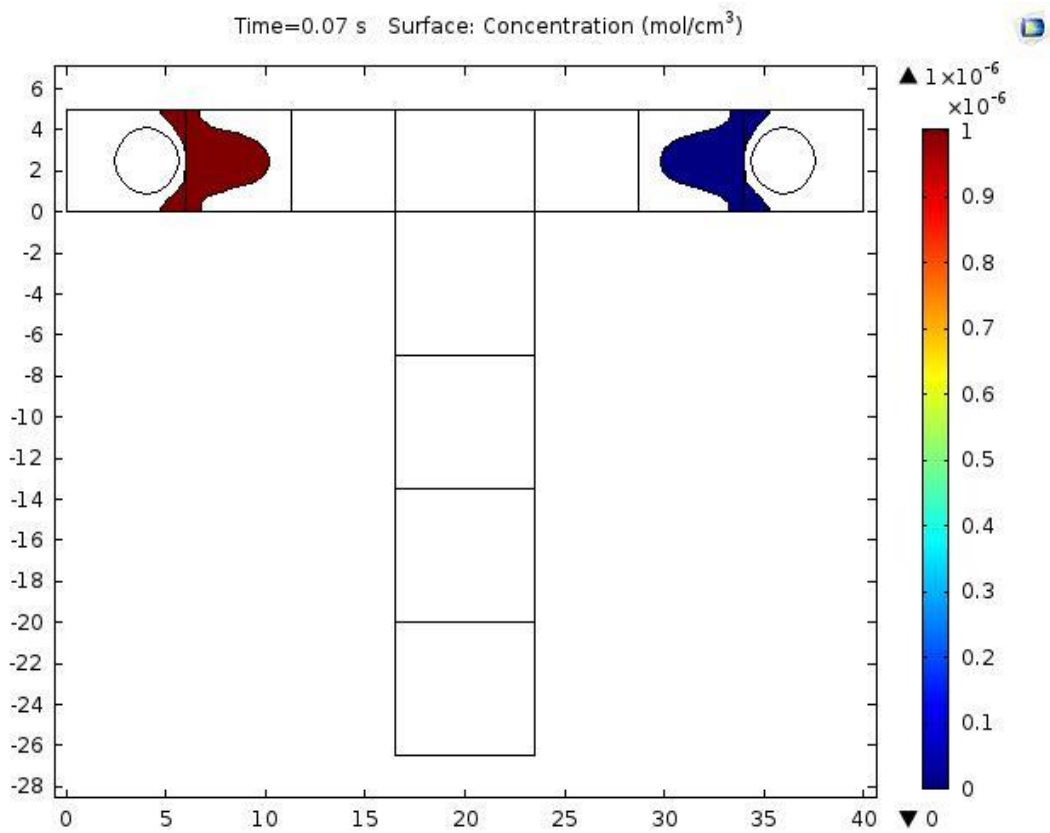
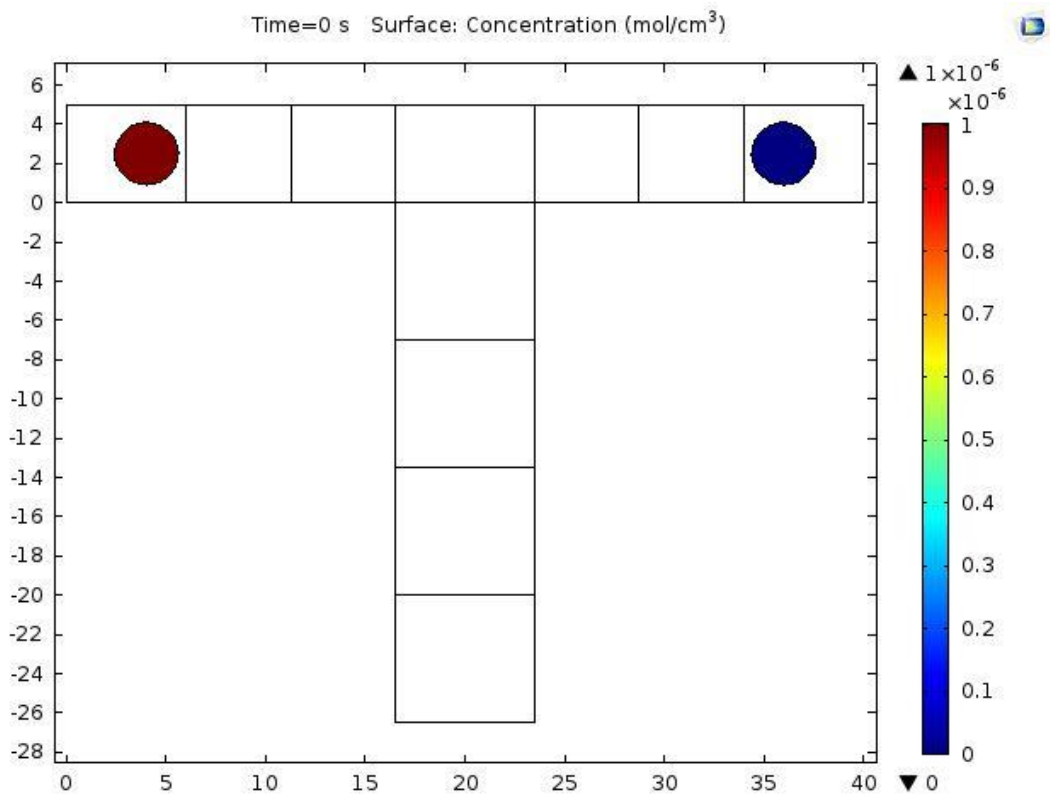
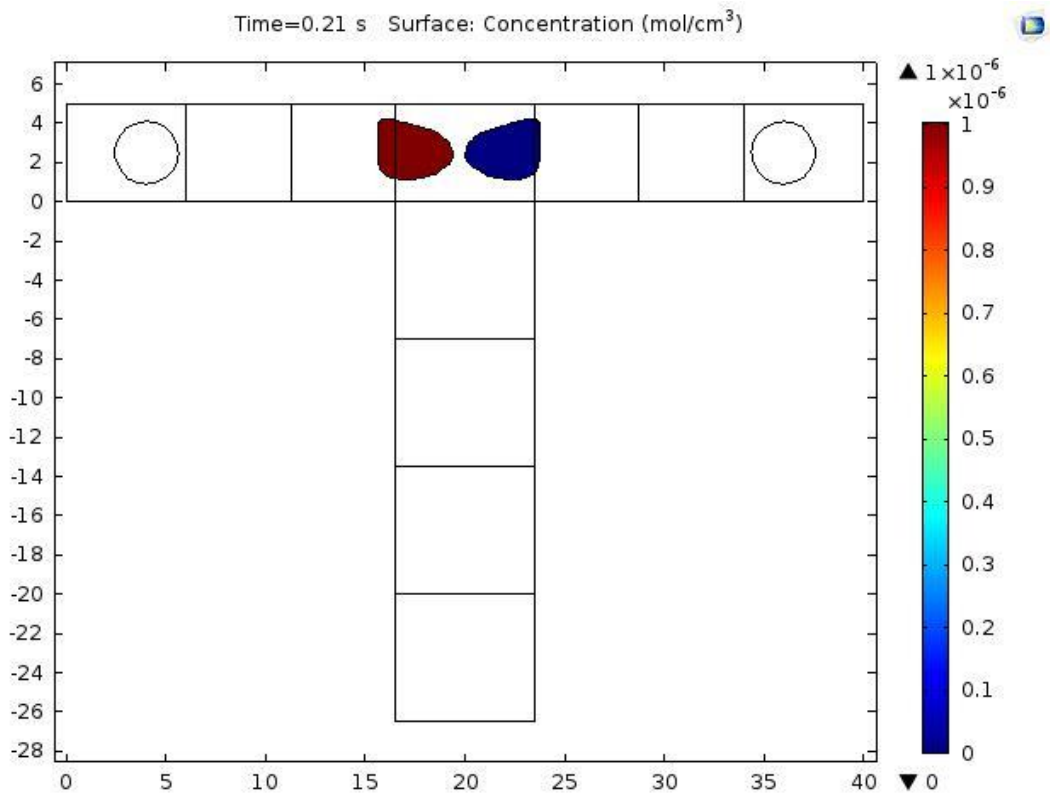
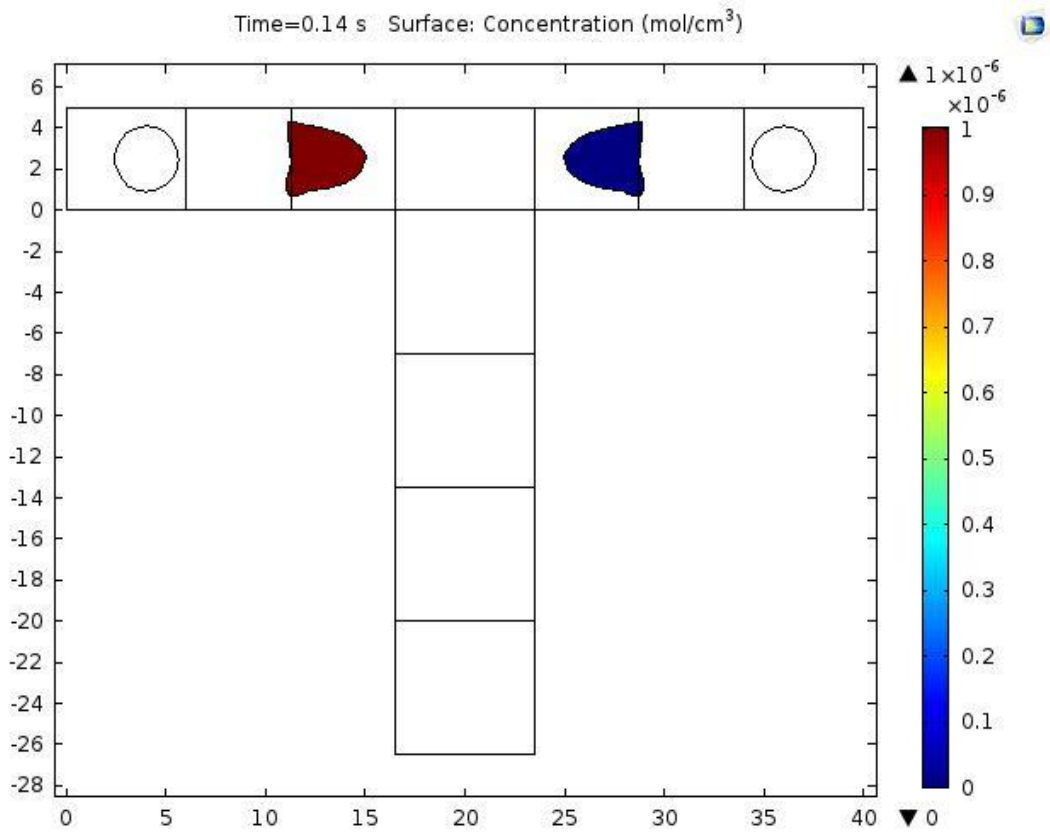
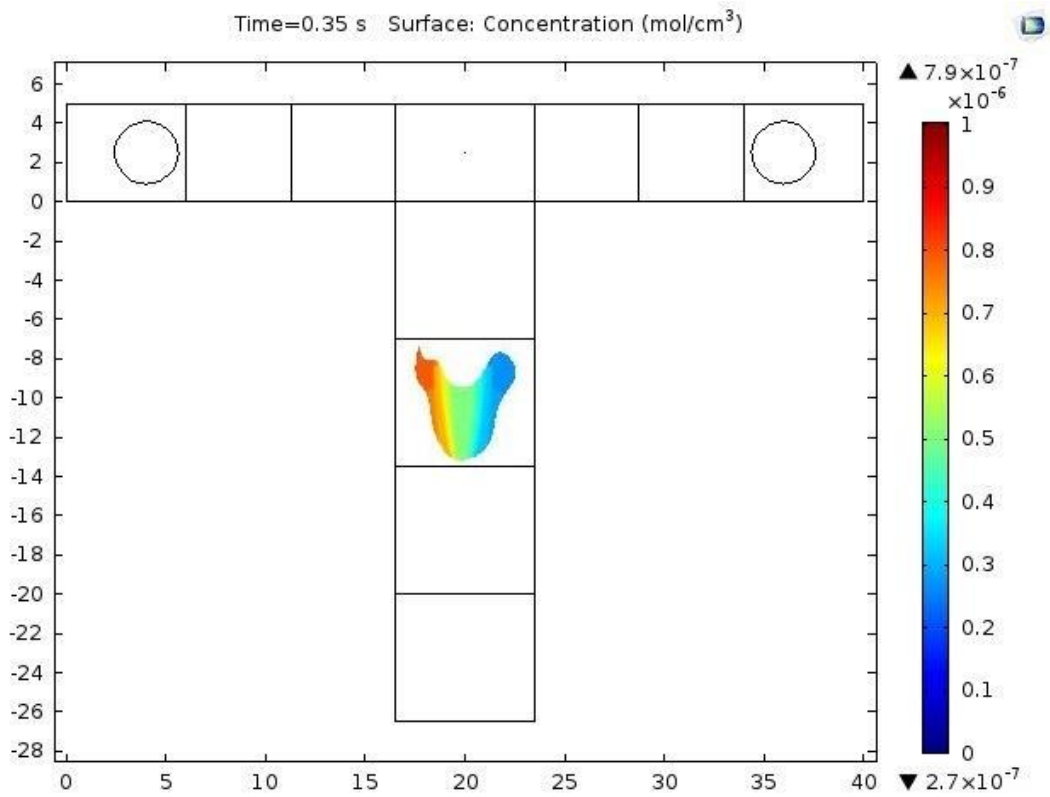
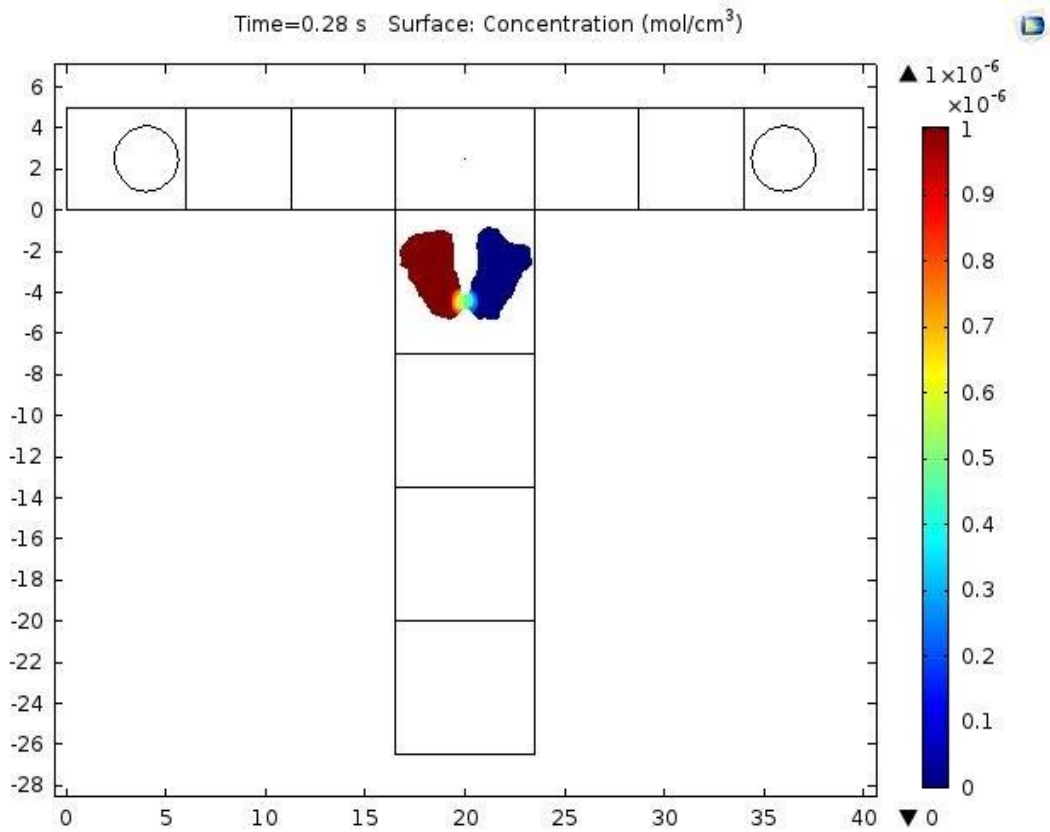


Figure 20: Contact angle simulation correspond to 0, 12.7, 17.5 V respectively
 **Error! Bookmark not defined.**

Droplet transport and mixing using the concept of Brochard's model and Lippmann-Young equation is successfully simulated on COMSOL Multiphysics platform. It has tremendous application in diverse fields. Figure 21 demonstrates the transport and mixing of two discrete droplet having dissimilar concentration at different time scale. RGB color bar demos the concentrations of the fluids, whereas in top it records the maximum concentration and in bottom the minimum concentration. The surface velocity from navier stokes equation has been coupled with convection diffusion equation to mix two fluid having dissimilar concentrations.







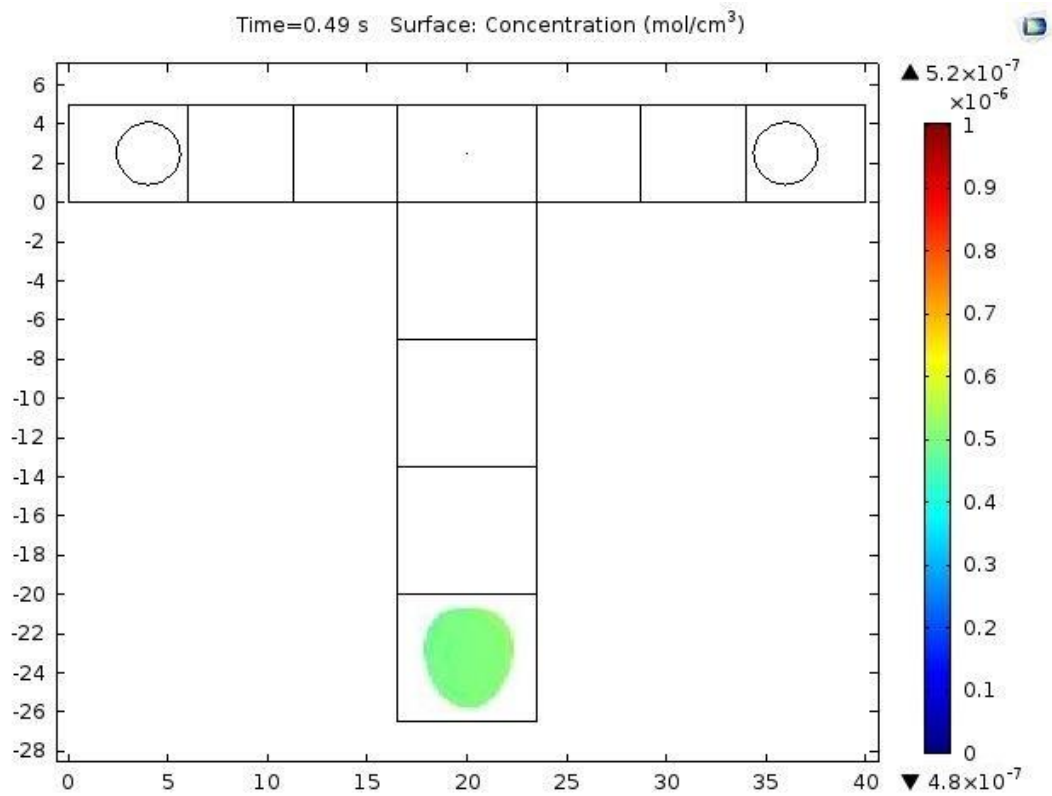
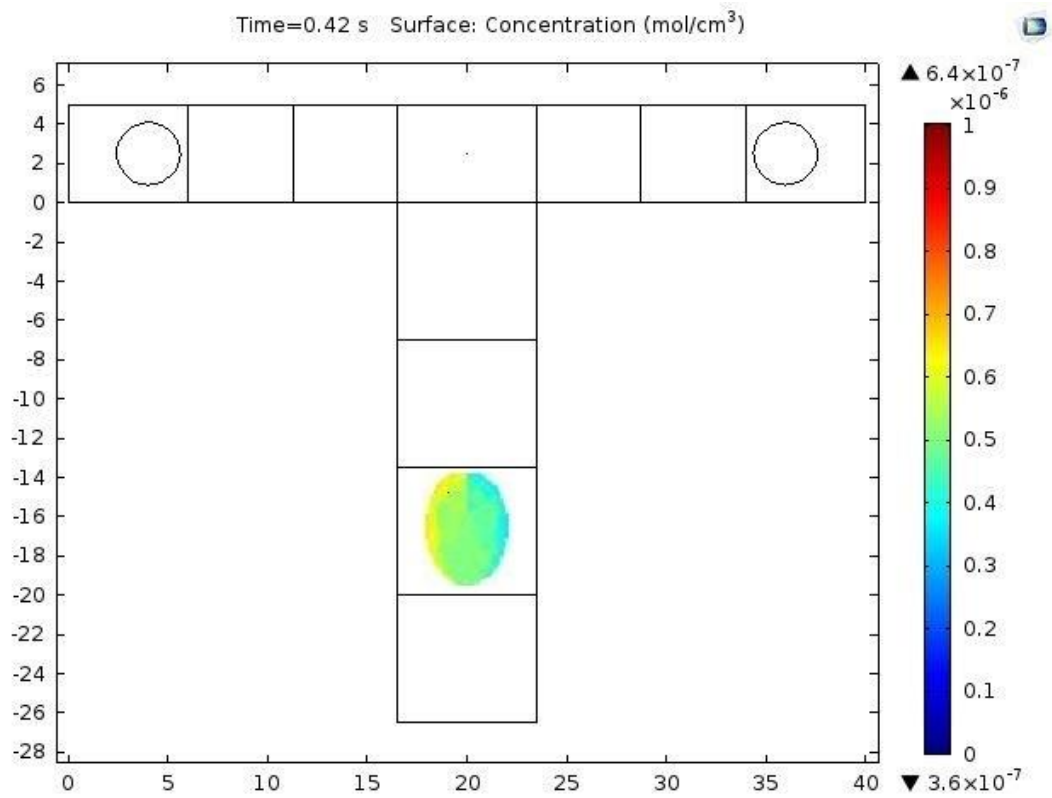


Figure 21: Recorded maximum and minimum concentrations i.e (1,0), (1,0), (1,0), (1,0), (1,0), (0.79,0.27), (0.64, 0.37) and (0.52,0.48) mol/m³ at time 0.07, 0.14, 0.21, 0.28, 0.35, 0.42 and 0.49 Sec respectively..... **Error! Bookmark not defined.**

The resultant recorded maximum and minimum concentrations are presented in below tables for 17.5V and 12.7V respectively. The resultant recorded maximum and minimum concentrations are (1,0), (1,0), (1,0), (1,0), (1,0), (0.79,0.27), (0.64, 0.37) and (0.52,0.48) mol/m³ at time 0.07, 0.14, 0.21, 0.28, 0.35, 0.42 and 0.49 Sec respectively Its appearances deviation of ± 0.2 with expected average concentration i.e 0.5 mol/m³.

Table 3: Concentration profile with respect to time at 17.5 V.

Time (S)	Minimum Concentration (mol/m³)	Maximum Concentration (mol/m³)
0	0	1
0.07	0	1
0.14	0	1
0.21	0	1
0.28	0.27	0.79
0.35	0.36	0.64
0.42	0.44	0.56
0.49	0.48	0.52

Table 4: Concentration profile with respect to time at 12.7V.

Time (S)	Minimum Concentration (mol/m³)	Maximum Concentration (mol/m³)
0	0	1
0.07	0	1
0.14	0	1
0.21	0	1
0.28	0.15	0.9
0.35	0.20	0.83
0.42	0.23	0.79
0.49	0.24	0.77

Table 5: Differences of maximum and minimum concentration at voltages.

Time (S)	12.7V	14.3V	15.9V	17.5V
0.21	1	1	1	1
0.28	0.75	0.67	0.59	0.52
0.35	0.63	0.51	0.39	0.28
0.42	0.56	0.41	0.26	0.12
0.49	0.53	0.36	0.2	0.04

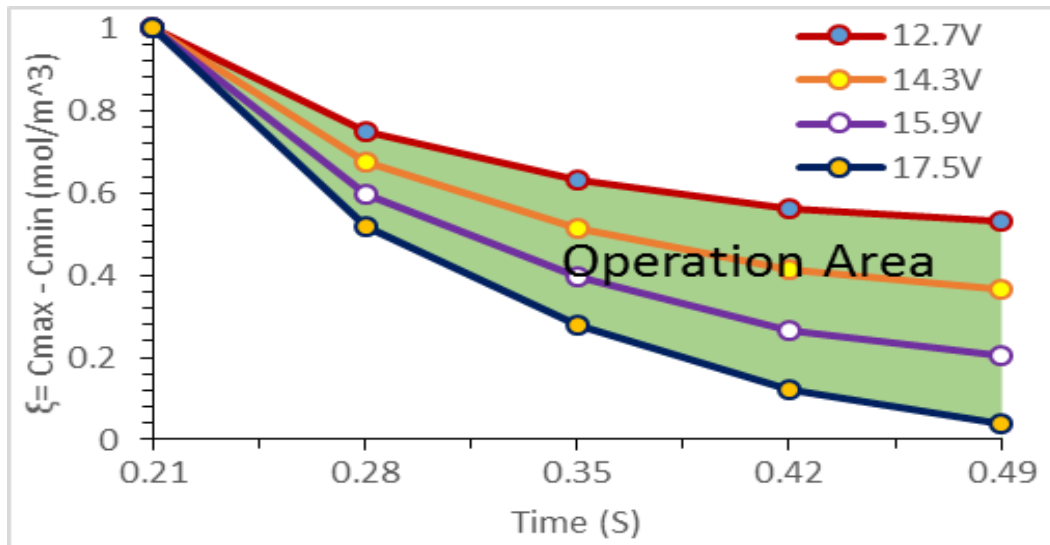


Figure 21: Mixing efficiency plot and operation area **Error! Bookmark not defined.**

The efficiency plot with $C_{max} - C_{min}$ shown in Figure 21. Different simulation has been carried out with respect to voltages to find out the operational area under which the experimental must be conceded. The green shaded area on efficiency plot shows the operational area. It also present critical voltage for this simulation is 12.5 V, whereas in previous literature, 15V has been reported [31]. Experiment is not possible to perform above 17.5V science the shape of the droplet is distorting and missing the track which has been illustrated in Figure 17. Table-2 shows the change in contact angle and relative change in contact angle with respect to voltage respectively which is plotted in Figure 18. Critical and saturated shape of the droplet illustrated in Figure 15 where the white line present the unbiased shape of the droplet. Whereas the distorted shaper of the droplet are in Figure 17 while operating in saturation zone i.e. > 17.5V. Table 3 and 4 recorded the minimum and maximum concentration for 12.7 and 17.5 V. Differences of maximum and minimum concentration are calculated on table 5. Mixing efficiency plot shown in figure 21, which represent the operational area for operating voltage value.

The rainbow color bar is screening in Figure 22 for electric field, which demonstrate only for one time scale i.e at initial switching electrode. And Figure 23 for velocity profile of the droplet.

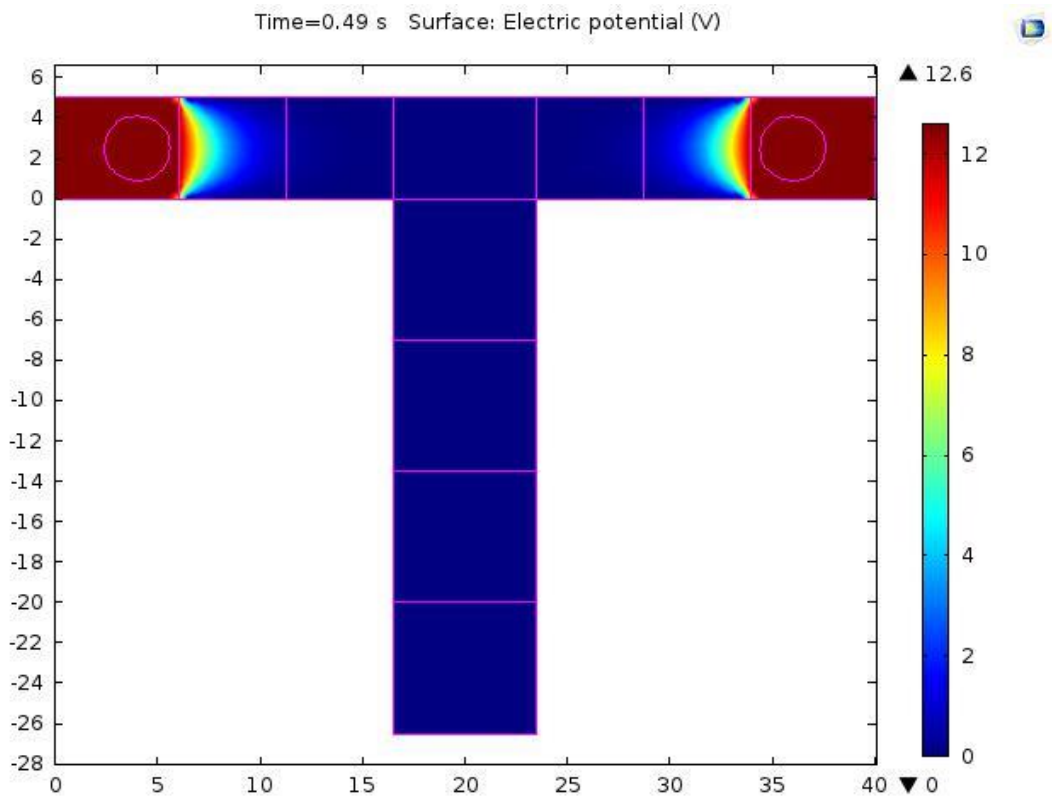


Figure 22: The electric field simulation of 1st and 2nd electrodes.....**Error! Bookmark not defined.**

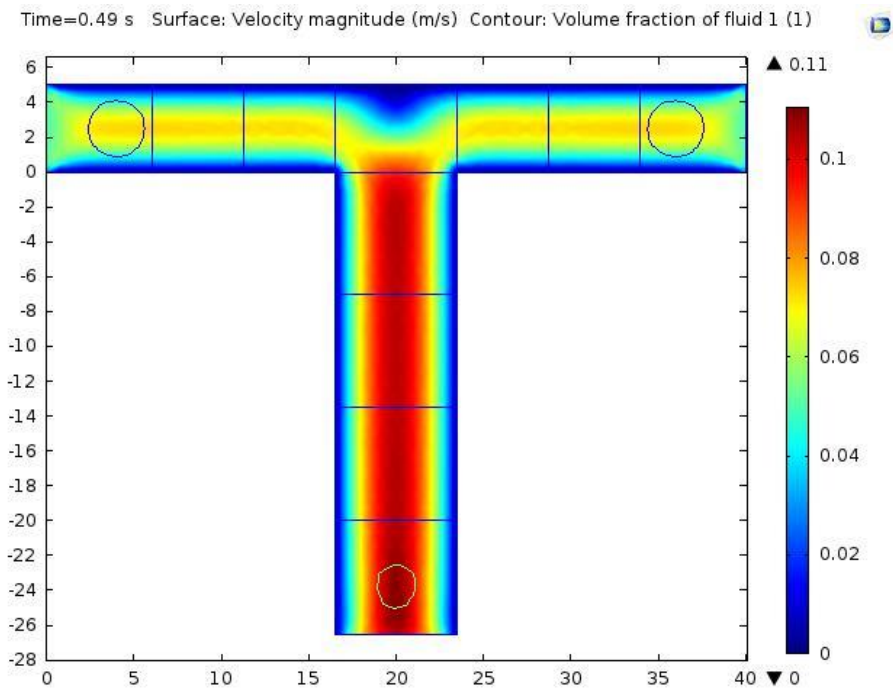


Figure 23: Velocity profile of the droplet..... **Error! Bookmark not defined.**

3-D packet transform of droplet by switching the voltage has been simulated, without surface modification as below.

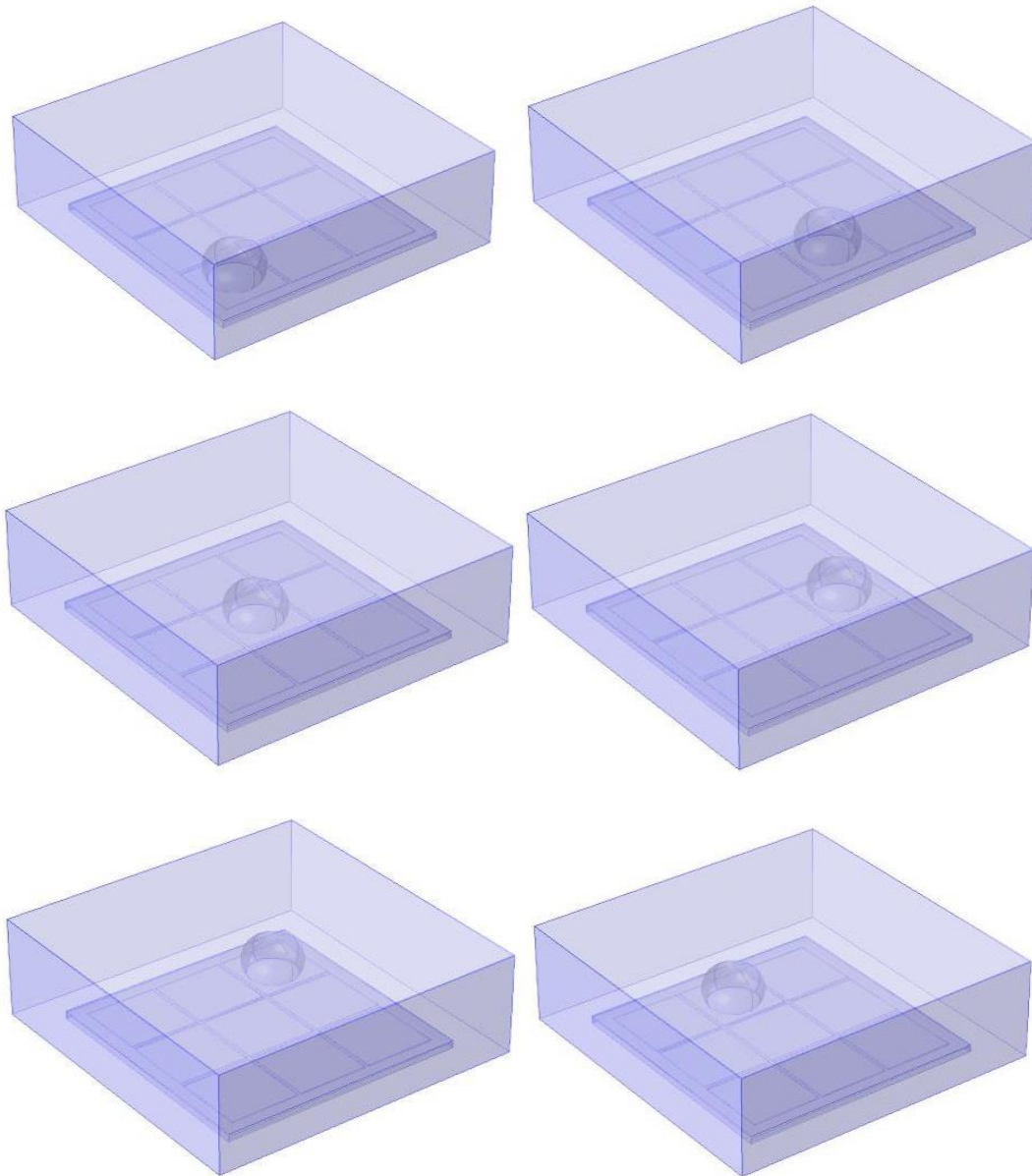
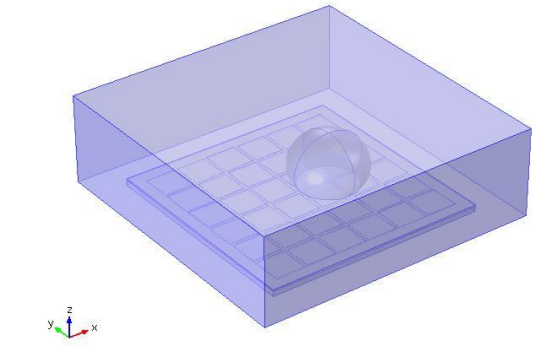
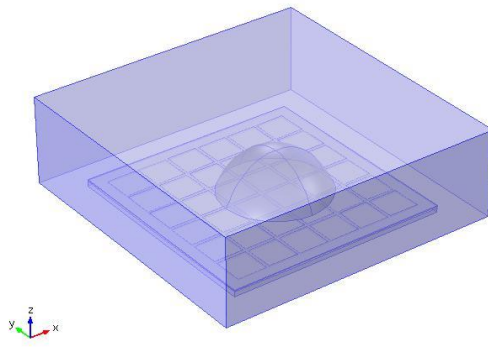
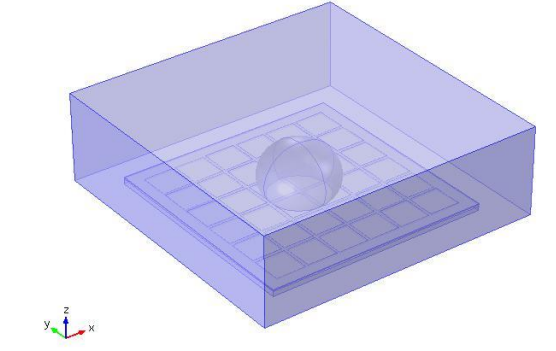
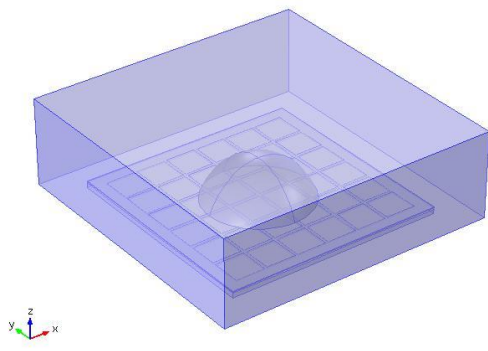
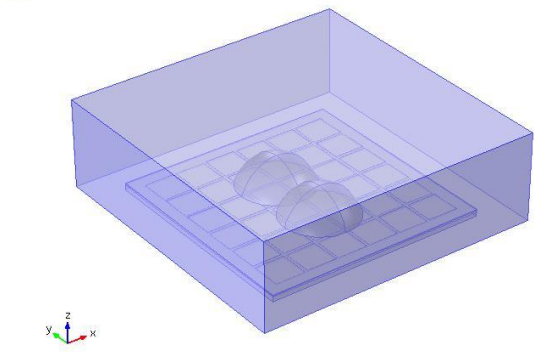
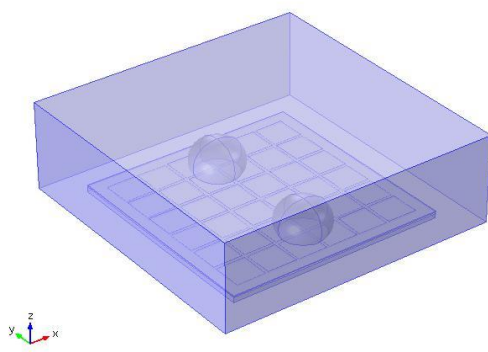
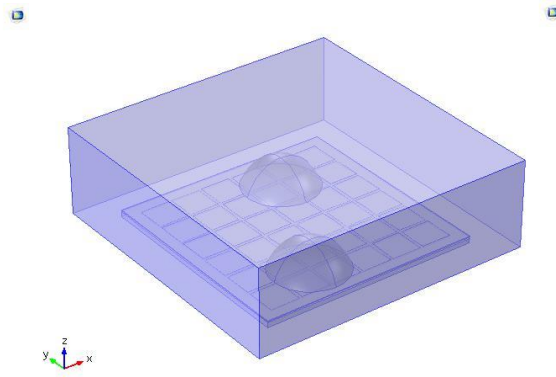
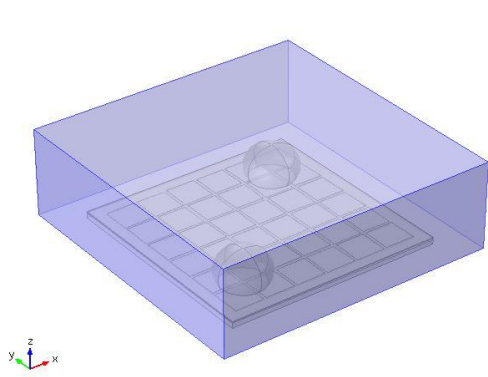


Figure 24: 3-D packet transform of droplet **Error! Bookmark not defined.**

The 3-D mixing of two different concentrated fluid is simulated on 6×6 array of electrodes platform, where droplets are deforming during transformation.



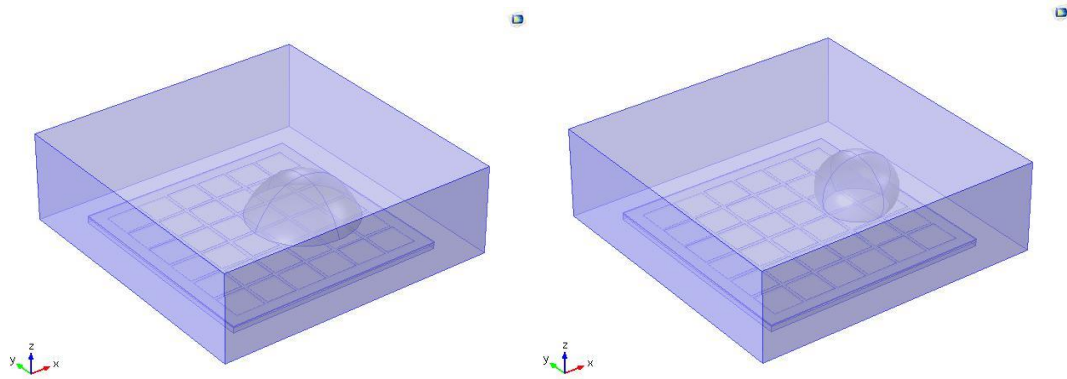


Figure 25: 3-D Droplet transform and mixing ... **Error! Bookmark not defined.**

The result shows, 3-D mixing efficiency is almost matching with 2-D mixing. The 2-D mixing efficiency have the error tolerance of ± 0.02 , whereas the 3-D mixing have error tolerance of ± 0.03 .

Conclusion

In the present work, we have calculated the 2-D & 3-D droplet change in contact angle with respect to voltage and time. Also we have simulated the time dependent transport of a single droplet over a one-dimensional electrode array with respect to time and space. In addition, we have simulated the 2-D & 3-D droplet mixing of two droplet over two dimensional platform with respect to time and spacer by proper switching mechanism. The efficient switching mechanism has obtained by coupling matlab with comsol. Using the information gathered from the above simulation, the complex systems can be over simplified to address the challenges we mention in this paper.

The LoC does not involve with animal testing and human trial for pharmaceutical research which makes the process cost effective and time saving as well. The idea of home health care device can be extended for applications like RBC count for cancer patient.

The simulated result will also help for farther study, which enabling the integration of multiple subsystem modules into an automated NGS library sample preparation system. This emerging technology combines electronics with biology to open new application areas such as point-of-care diagnosis, on-chip DNA analysis, and automated drug discovery.

References

- [1] K. Chakrabarty, "Automated Design of Microfluidics-Based Biochips: Connecting Biochemistry to Electronics CAD" IEEE International conference on computer design, San Jose, CA, Oct. 1-4, 2007, 93-100.
- [2] Baviere R, Boutet J, Fouillet Y, (2008) "Dynamics of droplet transport induced by electrowetting actuation," *Microfluidics nanofluid* 4:287–294.
- [3] V. Srinivasan, V. Pamula, M. Pollack, and R. Fair, "A digital microfluidic biosensor for multianalyte detection," in *Proc. IEEE 16th Annu. Int. Conf. Micro Electro Mech. Syst.*, 2003, pp. 327–330.
- [4] R. Fair, "Digital microfluidics: Is a true lab-on-a-chip possible?," *Microfluid. Nanofluid.*, vol. 3, no. 3, pp. 245–281, Jun. 2007.
- [5] S. K. Cho, H. Moon, and C. J. Kim, "Creating, transporting, cutting, and merging liquid droplets by electrowetting-based actuation for digital microfluidic circuits," *J. Microelectromech. Syst.*, vol. 12, no. 1, pp. 70–80, Feb. 2003.
- [6] Y.-H. Chang, G.-B. Lee, F.-C. Huang, Y.-Y. Chen, and J.-L. Lin, "Integrated polymerase chain reaction chips utilizing digital microfluidics," *Biomed. Microdevices*, vol. 8, no. 3, pp. 215–225, Sep. 2006.
- [7] R. Digilov, Charge-Induced Modification of Contact Angle: The Secondary Electrocapillary Effect, *Langmuir*, 2000, 16, 6719–6723.
- [8] C.Suman, R.Mittal, "Droplet dynamics in a microchannel subjected to electrocapillary actuation," *Journal of Applied Physics*, 101, 104901 (2007).
- [9] C. Buie, D. Kim, et al, "An electro-osmotic fuel pump for direct methanol fuel cells," *Electrochem. Solid-State Lett.*, vol. 10, no. 11, pp. B196–B200, 2007
- [10] M. Schneider, Z. Guttenberg, et al, "An acoustically driven microliter flow chamber on a chip (μ FCC) for cell–cell and cell–surface interaction studies," *ChemPhysChem*, vol. 9, no. 4, pp. 641–645, Mar. 2008.
- [11] Wang W, Jones TB (2011) Microfluidic actuation of insulating liquid droplets in a parallel plate device. *J Phys Conf Ser* 301:012057.
- [12] N. Pamme, "Magnetism and microfluidics," *Lab Chip*, vol. 6, no. 1, pp. 24–38, 2006.
- [13] W. H. Huang, F. Ali, Z. L. Wang, and J. K. Cheng, "Recent advances in single-cell analysis using capillary electrophoresis and microfluidic devices," *J.*

- Chromatogr. B, Anal. Technol. Biomed. Life Sci., vol. 866, no. 1/2, pp. 104–122, Apr. 2008.
- [14] The Nano World Cancer Day 2014, The ETP Nanomedicine and its partners, reported by Centre for Drug Research (CDR), University of Helsinki.
- [15] Debanjan Das, Shiraz Sohail, et al. “Voltage and Capacitance Analysis of EWOD System Using COMSOL” COMSOL conference’2011
- [16] M. G. Lippmann, *Ann. Chim. Phys.* 5, 494 (1875)
- [17] Kedzierski, J., S. Berry, et al. New Generation of Digital Microfluidic Devices. *Microelectro mechanical Systems, Journal of* 18.4 (2009): 845-851. ©2009 Institute of Electrical and Electronics Engineers
- [18] V. Peykov, A. Quinn and J. Ralston, *Electrowetting: A Model for Contact-Angle Saturation, Colloid Polym. Sci.*, 2000, 278, 789–793.
- [19] Thomas Young, “An essay on the cohesion of fluids”, *Phil. Trans. Roy. Soc.*, vol 95, pp. 65-87(1805)
- [20] Hyejin Moon, Sung Kwon Cho, et al. “Low Voltage Electrowetting-on-Dielectric” *Journal of Applied Physics* Vol. 92, no. 7.
- [21] T. A. Sammarco and M. A. Burns, “Thermocapillary pumping of discrete drops in microfabricated analysis devices,” *AIChE J.*, vol. 45, no. 2, pp. 350–366, 1999.
- [22] Roland Bavière, Jérôme Boutet, Yves Fouillet, “Dynamics of droplet transport induced by electrowetting actuation”, *Microfluidics and Nanofluidics*, May 2007, Volume 4, Issue 4 , pp 287-294.
- [23] Walker, S. W.; Shapiro, B.; Nochetto, R. H. Electrowetting with contact line pinning: Computational modeling and comparisons with experiments. *Phys. Fluids* 2009, 21.

- [24] Y. C. Lin, K. C. Chuang, T. T. Wang, C. P. Chiu, and S. K. Fan, "Integrated digital and analog microfluidics by EWOD and LDEP," in Proc. 1st IEEE Int. Conf. NEMS, 2006, pp. 1414–1417.
- [25] Liguo Chen, Xiaowei Xu et al., "Simulation and experimental verification of driving mechanism for a microfluidic device based on electrowetting-on-dielectric", International conference on Manipulation Manufacturing and Measurement on the Nanoscale, 26-30 August 2013.
- [26] S. K. Cho, H. Moon, and C-J. Kim, "Creating, transporting, cutting, and merging liquid droplets by electrowetting-based actuation for digital microfluidic circuits," *Journal of Microelectro-mechanical Systems*, vol.12, no.1, pp. 70-80, Feb 2003.
- [27] De Gennes P-G, Brochard-Wyart F, Que´re´ D (2002) *Gouttes, bulles, perles et ondes*. Collection e´chelles, Edition Belin Paris.
- [28] T. Ho. K. Chakrabarty and P. Pop "Digital microfluidic biochips: Recent research and emerging challenges", Proc. CODES+ISSS, pp.335 -343 2011
- [29] F. Su, K. Chakrabarty, and R. B. Fair, "Microfluidics based biochips: Technology issues, implementation platforms, and design-automation challenges," *IEEE Trans. on CAD*, pp. 211–223, 2006.
- [30] R. B. Fair, A. Khlystov, T. D. Taylor, V. Ivanov, R. D. Evans, P. B. Griffin, V. Srinivasan, V. K. Pamula, M. G. Pollack, and J. Zhou, "Chemical and biological applications of digital-microfluidic devices," *IEEE Des. Test Comput*, vol. 24, no. 1, pp. 10–24, Jan.–Feb. 2007
- [31] H. Moon, S. Kwon et al., "Low voltage electrowetting-on-dielectric". *Journal of applied physics*, Vol. 92, No. 7.
- [32] D. Chatterjee, B. Hetayothin, et al., "Droplet-based microfluidics with nonaqueous solvents and solutions",